The Contingency of Metabolic Pathway Evolution on Pre-existing Enzymes

by

Lauren Celeste Phillips

Molecular, Cellular, and Developmental Biology, University of Colorado at Boulder

08. Apr. 2025

Committee Members:

Dr. Shelley Copley, thesis advisor, Molecular Cellular Developmental Biology

Dr. Soyeon Park, Molecular Cellular Developmental Biology

Dr. Natalie Ahn, Biochemistry

Abstract

Phillips, Lauren Celeste

The Contingency of Metabolic Pathway Evolution on Pre-existing Enzymes

Thesis directed by Professor Shelley D. Copley (Ph. D)

The evolution of metabolic pathways has provided life an avenue to survive environmental changes and has contributed to the diversity of life present today. Metabolic pathways are responsible for all the energy processing and chemical synthesis and breakdown of compounds in an organism. The evolution of metabolic pathways is currently best characterized through bioinformatic evidence by the patchwork model. The patchwork model describes how the formation of novel metabolic pathways occurs by patching together promiscuous reactions of enzymes. Little is currently known about how the process normally occurs, why some pathways arise and not others, and what dictates the evolutionary trajectory of a novel metabolic pathway. Prior work in the Copley lab created a model system to study metabolic pathway evolution using the synthesis pathway of pyridoxal 5′-phosphate (PLP) in γ-proteobacteria. An essential gene in the pathway, *pdxB,* was deleted in *Escherichia coli*, *Aliivibrio fischeri*, *Pseudomonas putida*, *Acinetobacter baylyi*, and *Salmonella enterica* followed by laboratory evolution in minimal medium. The organisms all evolved to restore PLP synthesis. To understand the differences in PLP synthesis restoration across the organisms, I fully characterized the evolved PLP synthesis pathway in *A. fischeri*. This provided insight into how the mutations that arose during evolution allowed for PLP synthesis to increase to physiologically relevant levels. In collaboration with other researchers in the Copley lab, I found that organisms can take different routes to restore PLP synthesis dependent on their repertoire of enzymes. To study what factors influenced the evolutionary

trajectory of the organisms, I conducted enzymatic assays of an enzyme critical in the restoration of PLP synthesis (3-phosphoglycerate dehydrogenase, SerA) in the majority of studied strains. I revealed significant differences amongst the promiscuous activities of SerA enzymes across organisms and showed that the promiscuous activities of SerA influenced the mechanism for restoration of PLP synthesis. These results provide insight into the process of metabolic pathway evolution and reinforce the contingency of metabolic pathway evolution on pre-existing enzymes.

Table of Contents

I. Introduction……………………………………………………………………………1

Early models of metabolic pathway evolution………………………………………… 3

The patchwork model……………………………………………………………….. 5

Enzyme promiscuity………………………………………………………… 5

The evolution of metabolic pathways through the patchwork model……………5

The vitamin B6 synthesis pathway in γ-proteobacteria as a model system for

Metabolic pathway evolution……………………………………………………7

Multiple organisms can evolve to synthesize PLP………………………………………9

II. Characterization of an evolved PLP synthesis protopathway in *Aliivibrio fischeri*……. 11

Introduction……………………………………………………………………………11

A. fischeri evolution identifies genes that are mutated in multiple lineages……………11

Δ*pdxB A. fischeri* evolved a version of protopathway 1 to synthesize PLP …………….12

Mutations in *yidA* and *serA* helped restore PLP synthesis during evolution of

A. fischeri Δ*pdxB*………………………………………………………………….. 24

Mutations in *yidA* could increase flux into PLP synthesis……………………… 24

Mutations in *serA* contributed to PLP synthesis in Δ*pdxB A. fischeri* strains……25

Discussion……………………………………………………………………………26

III. Differences between the promiscuous activities of 3-phosphoglycerate

dehydrogenase orthologous and their influence on bacterial evolution after deletion

of *pdxB*…………………………………………………………………………………27

Introduction……………………………………………………………………………27

SerA kinetic assay scheme………………………………………………………… 30

Enzymatic activities of SerA enzymes vary across species……………………………32
Promiscuous activities of wild-type SerA enzymes influence the mechanism for restoration of PLP synthesis…...…………………………………………………… 33
Mutations in *serA* increase SerA promiscuous activity with erythronate or 4PE…35
Some mutations in *serA* affect feedback inhibition of SerA by serine……………35
The promiscuous activities of SerA influence the accessibility of various mechanisms for restoration of PLP synthesis after deletion of *pdxB*………… 36
Discussion………………………………………………………………………………37
IV. Conclusion………………………………………………………………………41
Outstanding questions…………………………………………………………………42
Is there a contingency on pre-existing enzymes?…………………………………42
How do rate-limiting enzymes influence the evolution of metabolic pathways?.. 42
The impact of metabolic pathway evolution………………………………………43
V. Methods……………………………………………………………………………45
General methods……………………………………………………………………..45
Reagents……………………………………………………………………………..45
Bacterial growth……………………………………………………………………..45
Gibson Assembly……………………………………………………………………46
Splicing by overlap extension (SOE) PCR………………………………………..48
Colony PCR………………………………………………………………………….49
A. fischeri methods…………………………………………………………………..51
Minimal medium……………………………………………………………………51
Growth environment…………………………………………………………………52

Antibiotic concentrations……………………………………………………………..52

Amino acid supplementation…………………………………………………………52

A. fischeri genetic manipulation…………………………………………………………..54

Creating a *tfoX* overexpressing strain………………………………………………54

Linear fragment deletion protocol ………………………………………………………55

Synthesis of 4PE…………………………………………………………………………………57

Protein purification…………………………………………………………………………….58

Protein expression……………………………………………………………………..58

purification and affinity column preparation…………………………………………60

Purification of ThrB……………………………………………………………………………60

Purification of DenK…………………………………………………………………………...62

Purification of D2HGDH……………………………………………………………………64

Purification of ETFAB……………………………………………………………………….65

Purification SerA……………………………………………………………………………..66

Kinetic assays of ThrB………………………………………………………………………67

Kinetic assays of SerA……………………………………………………………………….68

VII. References…………………………………………………………………………………71

VIII. Appendix…………………………………………………………………………………75

Tables……………………………………………………………………………………………75

Figures…………………………………………………………………………………………83

Glossary

Abbreviation	Full name
AspC	aspartate aminotransferase
DAP	diaminopimelic acid
DenK	D-erythronate kinase
DHOB	(3R)-3,4-dihydroxy-2-oxobutanoate
DtnK	D-threonate 4-kinase
HOPB	(3R)-3-hydroxy-2-oxo-4-phosphooxybutanoate
IPTG	isopropyl β- d-1-thiogalactopyranoside
PdxB	erythronate 4-phosphate dehydrogenase
PEP	phosphoenolpyruvate
PL	pyridoxal
PLP	pyridoxal 5'-phosphate
PN	pyridoxine
PP	protopathway
SerA	D-3-phosphoglyderate dehydrogenase
SerC	phosphoserine/phospohydroxythreonine aminotransferase
ThrB	homoserine kinase
4HT	4-phosphodydroxythreonine
4PE	4-phosphoerythronate
3PG	D-3-phosphoglycerate
4PHT	4-phospho-hydroxy-L-threonine

Chapter I

Introduction

All life has used evolution to endure significant environmental changes, allowing for the persistence of life for 4 billion years. The evolution of living organisms contributes to their ability to adapt to changes in the environment. Some of these changes occur in the alteration of metabolism (Fani and Fondi 2009). Metabolism encompasses all the processes by which living organisms process energy and replicate. There are two categories of metabolic processes. Catabolism is the degradation of molecules to access stored energy and essential atoms such as carbon and nitrogen. Anabolism utilizes the products created from catabolism and synthesizes building blocks of life including macromolecules, including proteins, lipids, nucleic acids and cofactors. (Judge and Dodd 2020; Scossa and Fernie 2020). These metabolic processes, referred to as primordial metabolism, were present in the last universal common ancestor (LUCA) (Fani and Fondi 2009), and since, many new pathways have emerged (**Figure 1**). The evolution of metabolic pathways has contributed to the present biological diversity and the study of them has become increasingly important with the rapidly changing environment today.

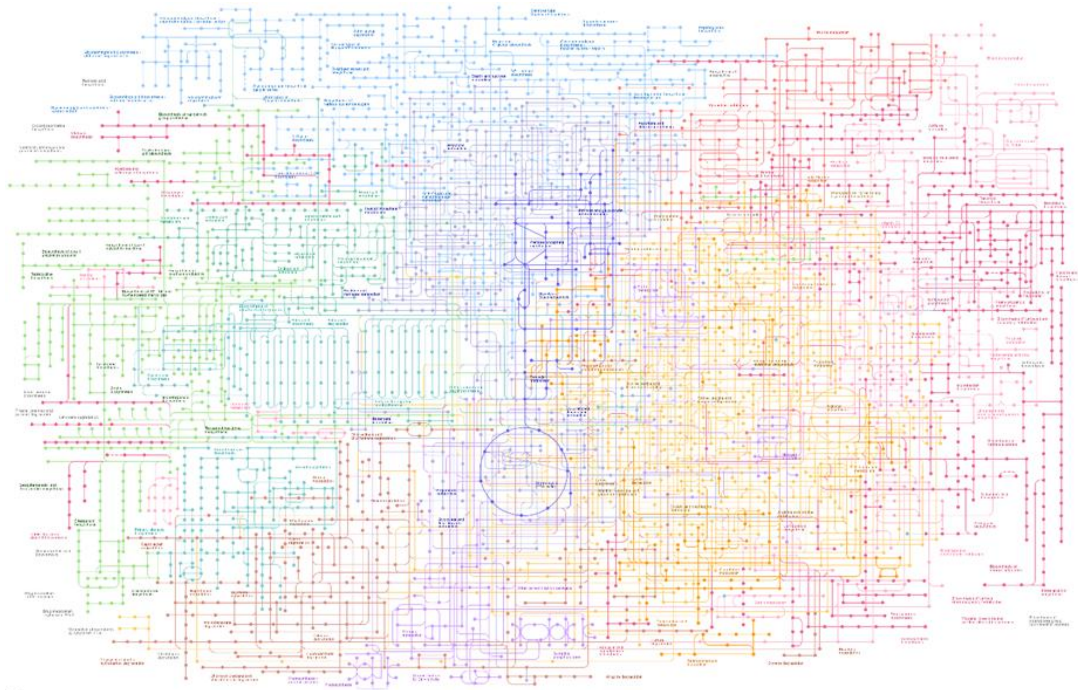

Figure 1. Metabolic pathway diagram reflects the vast quantity and complexity of metabolic pathways. Diagram created by Kanehisa Laboratories (Kanehisa and Goto 2000; Kanehisa 2019; Kanehisa et al. 2025).

The evolution of novel metabolic pathways is exploited today to help reduce the negative environmental impact of humans in recent years. The field of directed evolution, in particular, has explored the opportunities for utilizing metabolic processes for the environmentally friendly degradation and synthesis of compounds through the use of microbes (heterologous synthesis). The evolution of metabolic pathways affects this field by helping answer the questions why some metabolic pathways are more difficult to create than others, and what are the limits to new pathways that can be created?

This field also focuses on the model organism used and the potentials it can offer for metabolic pathway formation. One example is the use of cyanobacteria — photosynthetic bacterium — as a model organism to reduce the bacteria's primary energy source to solely light compared to glucose, often used for *Escherichia coli* (Ducat et al. 2011). In respect to a variety of model organisms, are there differences in metabolic pathway evolution across species, and is there a contingency of metabolic pathway evolution on pre-existing enzymes within an organism? I have explored these questions using biochemical, molecular biology and genetic methods to study the evolution of a novel metabolic pathway in a laboratory setting. Building from the prior work of laboratory evolutions of new metabolic pathways, I studied the mutations that arose during the evolution of a metabolic pathway, how they influenced the evolved pathway, and how this process was affected by the promiscuous activities of one critical enzyme.

This chapter defines the concept of enzyme promiscuity, describes two primary theories for metabolic pathway evolution, and introduces the model system used in the Copley lab and prior research to study the evolution of a novel metabolic pathway. Chapter II describes the characterization of an evolved metabolic pathway in *Aliivibrio fischeri* to support comparisons of metabolic pathway evolution between organisms. Chapter III analyzes an important enzyme for the evolution of the studied metabolic pathway and how it may have affected the evolutionary trajectories of multiple organisms. Chapters II – IV are summarized in the discussion providing insight into how metabolic pathways evolve. Chapter V describes the methods used in this work.

Early models of metabolic pathway evolution

Four primary models have been used to describe the evolution of metabolic pathways. These include the forward model, Granick's hypothesis, the shell hypothesis, and the patchwork model (Scossa and Fernie 2020). The Granick hypothesis describes metabolic pathway evolution having occurred in a forward, stepwise process (Scossa and Fernie 2020). In this model an ancestral organism had fewer enzymes than present today, and the enzymes only produced a certain number of products necessary for life (Lazcano and Miller 1999; Fani and Fondi 2009). Over time, novel enzymes arose that can convert products from the pre-existing enzymes to new metabolites.

This process continued over the course of the evolution of life, forming the metabolic pathways present today. A pathway that might have been created from this model is glycolysis, which has ten enzymes in one pathway and each intermediate product produced during the pathway is stable. This model requires intermediates to be stable and exist in organisms long enough for a novel enzyme to evolve and utilize the intermediate. This is a problematic model for many characterized pathways today that have unstable intermediates, which only exist in cells for a brief amount of time.

The retrograde model is one of the first models and associated each gene with only one gene product, one enzyme (Takemoto 2012). This model assumes the essential molecules for life existed in their usable forms as a "primordial soup" (Scossa and Fernie 2020). Changing environmental conditions reduced quantities of and access to some of these essential molecules. This created evolutionary pressure for novel enzymes to arise. Genes encoding enzymes duplicated and diverged to allow the synthesis of, now scarce, essential molecules from other, more abundant molecules (Scossa and Fernie 2020). Over time the accessibility to essential molecules decreased and the number of enzymes required to synthesize essential molecules increased, forming a network of metabolic pathways. Similar to the forward model, each intermediate in the pathways would need to be stable for it to have persisted in the environment and be utilized by novel enzymes.

A newer hypothesis was proposed by Morowitz in 1999 (Morowitz 1999; Scossa and Fernie 2020). This model proposes that the reverse citric acid cycle was the first chemical pathway to arise in organisms without the use of enzymes in prebiotic chemistry (Zimmermann et al. 2024). Carbon-based chemistries were the foundation of metabolic pathways and metal ions, and minerals to assist with catalysis (Schoenmakers et al. 2024). These catalysts were then replaced by enzymes.

In this model, different metabolic pathways were first introduced as shells/ chemical pathways, later followed by the rise of enzymes (Scossa and Fernie 2020).

The patchwork model

Enzyme Promiscuity

The patchwork model uses the assumption that enzyme specialization has increased overtime and enzymes early in the formation of life performed multiple functions, referred to as promiscuous enzymes (Lazcano et al. 1995). Enzyme promiscuity is the ability of an enzyme to catalyze secondary and physiologically irrelevant reactions in addition to the one for which it has evolved (Gupta 2016). Enzymes often physically position substrates in active sites using active site residues and ions to best facilitate the desired chemical reaction. Compounds with similar structures as the native substrate can sometimes bind the enzyme and undergo the same chemical reaction, which is referred to as a promiscuous activity of the enzyme.

The evolution of metabolic pathways through the patchwork model

The promiscuous activities of enzymes enabled them to perform new functions for the organism to process new and different molecules as the environment changed (Lazcano et al. 1995). Over time the genes encoding enzymes duplicated, allowing each gene copy to evolve independently over time with increased specialization of each enzyme (Scossa and Fernie 2020). In this model, the promiscuous activities of enzymes are patched together to form novel pathways and to provide necessary functions for life in a changed environment. This results in the ability for pathways to have unstable intermediates, like many pathways have today, because the intermediates are always used following their synthesis. The evolution of metabolic pathways following this model is not linear unlike the previously proposed models.

Currently, the patchwork model is the most supported model by bioinformatic data, which shows the involvement of pre-existing enzymes in novel metabolic pathways. This model has also been supported in vitro experiments through the characterization of novel pathways evolving in plastic-degrading bacteria (Zhang et al. 2022). The characterization of these pathways shows what pre-existing enzymes were utilized and capable of performing the promiscuous reactions in the evolved pathway. Additionally, the field of synthetic biology relies heavily on the model by patching together enzymes to create novel metabolic pathways for the heterologous synthesis or breakdown of a desired molecule.

While there is evidence to support the patchwork model, the process by which metabolic pathway evolution occurs remains unknown due to the complex nature of metabolic pathways. The metabolic network is highly interconnected, comprised of a multitude of pathways simultaneously impacting each other, and many factors contribute to the formation of a novel metabolic pathway. Some factors include the chemical composition of the environment, the availability of promiscuous enzyme activities, and the stochastic occurrence of mutations (Coton et al. 2022). Some of these factors can be observed through the laboratory evolution of a metabolic pathway, providing insight into how each factor contributed to the evolutionary trajectory. I have investigated the process of metabolic pathway evolution through studying the laboratory evolution of a metabolic pathway.

The vitamin B_6 synthesis pathway in γ-proteobacteria as a model system for metabolic pathway evolution

Vitamin B_6 (pyridoxal-5' phosphate, PLP) is an essential compound to life. It is used as a cofactor in many enzymatic reactions for cell wall synthesis, amino acid synthesis, neurotransmitter synthesis, and glycogen processing (Denise et al. 2023). Many organisms including humans acquire PLP through consumption and the use of salvage enzymes (Denise et al. 2023). Other organisms synthesize PLP using Pdx1 and Pdx2. The majority of proteobacteria synthesize PLP through the pathway depicted in **Figure 2**. The higher number of enzymes required to synthesize PLP suggests that the pathway is newer and was patched together to accommodate decreasing levels of PLP in the environment. Most proteobacteria still have salvage pathways, allowing them to consume other forms of vitamin B6 from the environment and convert them to PLP form for the (Denise et al. 2023). This has enabled the PLP synthesis pathway to be targeted for the study of metabolic pathway evolution.

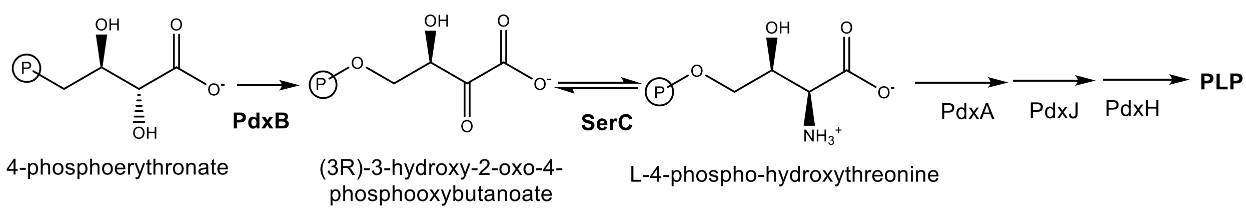

Figure 2. The canonical PLP biosynthesis pathway in γ-proteobacteria. The precursor to the pathway is D-erythrose 4-phosphate (E4P).

Dr. Juhan Kim, a former post-doc in the Copley lab, characterized the evolution of a metabolic pathway in *E. coli* using the PLP synthesis pathway (Juhan et al. 2019). The PLP synthesis pathway is essential in minimal medium in which the bacteria need to synthesize all of the complex molecules for life from a sole carbon source. He deleted the gene *pdxB* in the pathway in the *E. coli* BL21 strain. Following the deletion, growth of the *E. coli* Δ*pdxB* strain in minimal medium (M9, 0.4% glucose) was not abolished, but the growth rate was drastically reduced. This indicated to Kim et al. 2019 that, in the absence of PdxB, an alternative route for PLP synthesis was being used. He evolved six independent lineages of the *E. coli* Δ*pdxB* strain in M9, 0.4% glucose for 110-160 generations. The lineages were split after 20 generations and yielded 10 evolved lineages because two of the lineages failed to grow. Laboratory evolution was considered successful with an increased growth rate, suggesting that a novel pathway that restored PLP synthesis had evolved.

Following laboratory evolution, the genomes of individual clones from each population were sequenced to determine the mutations that arose during evolution and predict which mutations were critical for increasing PLP synthesis through a new pathway. A pathway was proposed and tested in one of the isolated clones named *Ec1* (JK1) (Juhan et al. 2019). The newly evolved pathway, now referred to as protopathway 1 (PP1), was verified by genomic and biochemical evidence. Both approaches confirmed that the enzymes involved in the restoration of PLP synthesis in *Ec1* include SerA, SerC, and ThrB (Kim et al. 2019). PP1 is a protopathway, defined as the earliest stage in the evolution of a novel metabolic pathway. The enzymes in a protopathway still perform their native functions and regulation of the pathway has not yet emerged. PP1 likely existed prior to laboratory evolution in *E. coli* and was utilized to support the slight growth of the *E. coli* Δ*pdxB* strain (Widney 2024). PP1 was then selected for during evolution and expression of the pathway increased.

The evolution of PP1 in Δ*pdxB E. coli* provided insights into the effect mutations can have on flux through a protopathway, activity of enzymes in the pathway, and overall metabolic pathway evolution. However, how does the process of metabolic pathway evolution vary between organisms? This question was explored through expanding this model system to other organisms (Widney 2024).

Multiple organisms can evolve to synthesize PLP

Four organisms including *Aliivibrio fischeri*, *Pseudomonas putida*, *Salmonella enterica* and *Acinetobacter baylyi*, were chosen to undergo the same evolutionary challenge as *E. coli* (Widney 2024). Dr. Karl Widney, a prior PhD student in the lab, deleted *pdxB* in *A. fischeri, P. putida* and *S. enterica* and conducted laboratory evolution of the strains in the appropriate minimal medium for each organism (**Figure 3**). Dr. Della Fixsen, a post-doc in the lab, deleted *pdxB* in *Acinetobacter baylyi* and, surprisingly, found that *A. baylyi* can restore PLP synthesis without evolution. The evolutionary trajectories taken by each organism reveal differences in their abilities to restore PLP synthesis. The evolved PLP synthesis pathways in each Δ*pdxB* organism have been studied to provide novel insight into how the process of metabolic pathway evolution occurs.

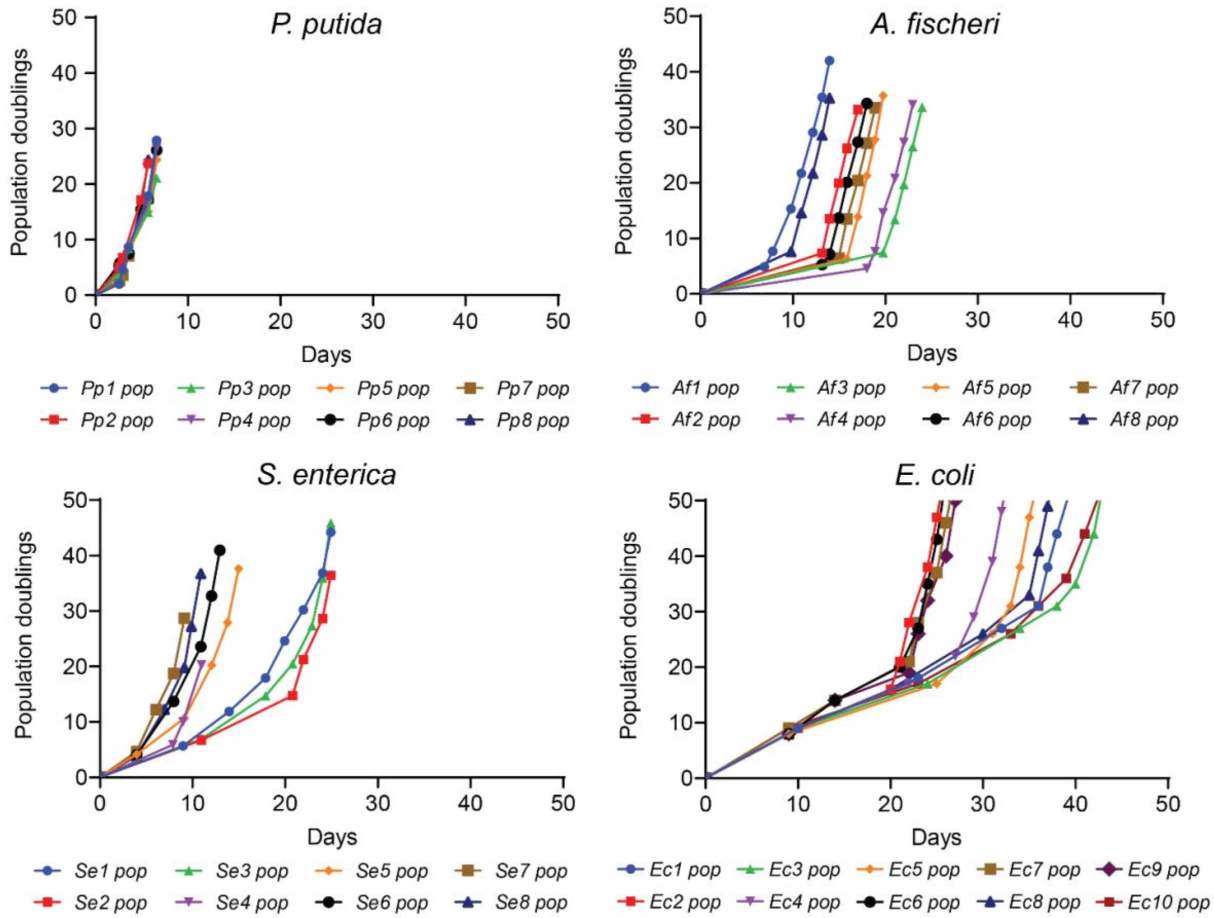

Figure 3. The length of evolution to restore PLP synthesis varies amongst organisms lacking PdxB. Δ*pdxB* organisms evolved in minimal medium and cultures were passaged at each graphed point. Created by Dr. Widney (Widney 2024).

Chapter II

Characterization of an evolved PLP synthesis protopathway in *Aliivibrio fischeri*

Introduction

Dr. Widney deleted *pdxB* in *Aliivibrio fischeri* ES114 and used directed evolution in Tris minimal medium (TMM) to evolve a novel PLP synthesis pathway in this strain. Eight flasks of Δ*pdxB A. fischeri* evolved for 10 - 25 days (**Figure 3**). Following the evolution, I studied two clones isolated from independently evolved lineages and determined how PLP synthesis was restored. I obtained genetic and biochemical evidence to confirm the involvement of multiple genes in the restoration of PLP synthesis. Genetic evidence reveals the essentiality of each tested gene for PLP synthesis in the evolved strains but does not demonstrate how the gene is involved in PLP restoration. Biochemical evidence confirms what reactions the enzyme can perform but does not guarantee the reaction occurs in vivo. A combination of genetic and biochemical evidence best supports which enzymes are involved in the restoration of PLP synthesis and what metabolic pathway evolved.

A. fischeri evolution identifies genes that are mutated in multiple lineages

Individual clones isolated from each of the eight evolved lineages were saved during evolution, and their genomes were sequenced. The sequencing results revealed mutations present in the different lineages and identified specific genes that often-acquired mutations (**Table 1**). *Af1*-*Af4* strains were isolated following the second passage and *Af5*-*Af8* strains were isolated following the fifth passage. Mutations in *rtxA2* likely do not directly contribute to PLP synthesis in Δ*pdxB*

A. fischeri. Mutations in *serA* and *yidA* arose most frequently. Strains isolated at the end of the second passage had mutations in one or the other of these genes, while strains isolated at the end of the fifth passage had mutations in both genes (**Table 1**). These data indicate important roles mutations in *yidA* and *serA* could have on PLP synthesis.

Table 1. Mutations from each Δ*pdxB A. fischeri* evolved lineage identify genes mutated in multiple lineages. A clone from each evolved lineage was isolated and sequenced to observe mutations that arose during evolution.

***A. fischeri* evolved strains**	**Gene description**	***Af1***	***Af3***	***Af2***	***Af4***	***Af5***	***Af6***	***Af7***	***Af8***
serA	D-3-phosphoglycerate dehydrogenase	L19F			C23Y	S296A	S296A	V330E	L19F, (+137/-58) (*rpiA/serA*)
yidA	Hydrolase, (sugar phosphatase)		Δ 44 aa	E83*		A238E	E83*	Δ3 aa	A112T
serC	Aminotransferase					C72Y			
mshE	MSHA biogenesis protein MshE							L573F	
glgB	1,4-alpha-glucan branching enzyme							V319V	
rtxA2	RTX calcium-binding sytotoxin RtA2					P861P	D865E &P861P		P861P
VF_1681	Coniferyl aldehyde dehydrogenase								G51G
VF_T0054/ VF_T0055	tRNA-Tyr/tRNA-Tyr					Intergenic (+6/-77)			

Δ*pdxB A. fischeri* evolved a version of protopathway 1 to synthesize PLP

The mutations that arose in *serA* and in *serC* during evolution of Δ*pdxB A. fischeri* suggested that PP1, which evolved during the Δ*pdxB E. coli* evolution, might have also emerged during this evolution. To test this hypothesis, I decided to work with two strains saved following the second passage (*Af1* and *Af2*). I deleted the genes encoding enzymes in PP1 (*serA*, *serC*, and *thrB*) from *Af1* and *Af2* and in wild-type *A. fischeri*. These genes are all essential in *A. fischeri* for growth in minimal medium. I deleted these genes in wild-type *A. fischeri* to identify the amino acids required to rescue growth in minimal medium. I then analyzed the effect of each gene deletion on growth of the evolved Δ*pdxB A. fischeri* strains in TMM containing glucose (0.4 %) and the appropriate supplements (**Table 2**). The maximum OD_{600} reached by *A. fischeri* in TMM is ~ 0.4, which does not allow for sufficient growth in a plate reader to obtain growth curves. (See further discussion in Chapter II.) Instead, I performed using spot dilutions on minimal medium agar plates, which do not provide quantitative results but are less affected by mutations that can arise during growth tests in liquid medium. Mutants can be distinguished as large colonies from the background growth of smaller colonies. My results are summarized in **Figure 4**.

Table 2. Amino acids required to support growth of A. fischeri strains with genomic deletions on TMM (0.4 % glucose). Amino acid concentrations used in A. fischeri were determined as described in Chapter IV.

Deletion	**Amino acid supplementation**
pdxB	10 µM pyridoxine
serA	1 mM serine
thrB	0.4 mM threonine
serC	10 mM glycine + 0.2 mM cysteine + 0.1 mM tryptophan
aspC	10 mM glycine + 4 mM aspartate + 0.04 mM phenylalanine, and 0.02 tyrosine

B.

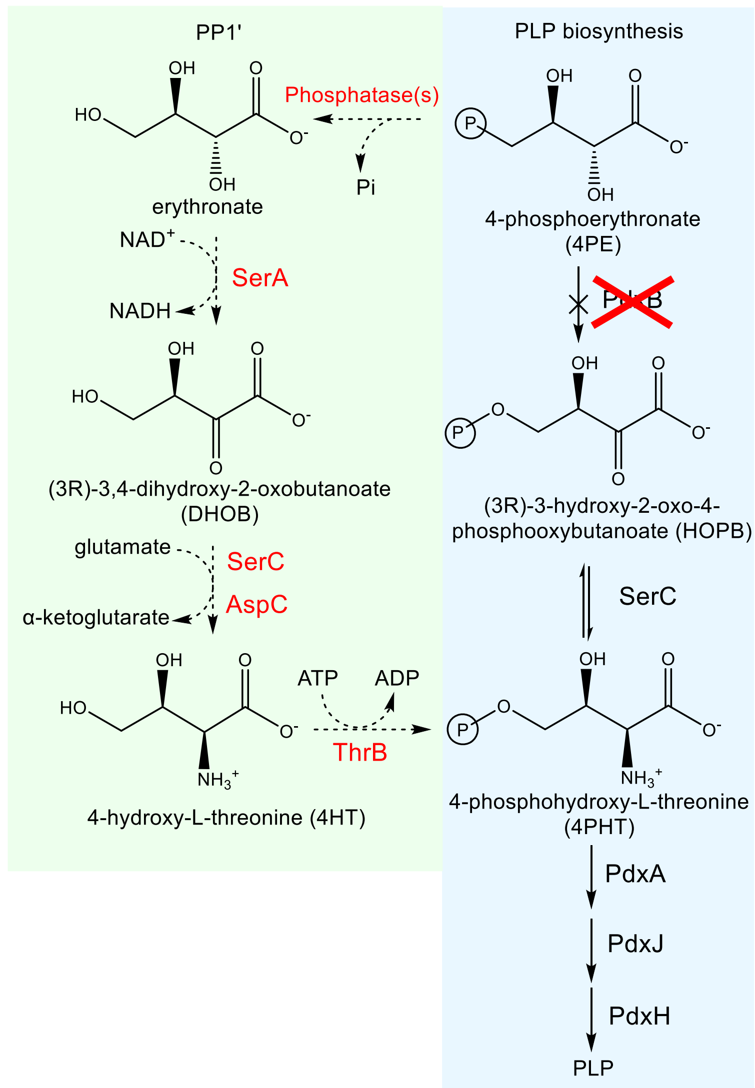

A.

Gene	*Af1*	*Af2*
Δ*serA*	***	
Δ*thrB*		
Δ*serC*		
Δ*aspC*		

Figure 4. **Δ*pdxB* *A. fischeri* evolved a version of PP1 to restore PLP synthesis.** A. The table depicts the level of growth of *Af1* and *Af2* strains on TMM plates with amino acid supplementation. Δ*serA* strains had 1 mM serine, Δ*thrB* strains had 0.4 mM threonine, Δ*serC* strains had 10 mM glycine + 0.2 mM cysteine + 0.1 mM tryptophan, and Δ*aspC* strains had 10 mM glycine + 4 mM aspartate + 0.04 mM phenylalanine, and 0.02 tyrosine. Black, abolished growth; grey, poor growth; light grey, reduced growth compared to growth on TMM medium with pyridoxine, which can be converted to PLP by a salvage pathway. B. The evolved *A. fischeri* PP1 is similar to *E. coli* PP1 except that two transaminases are involved in conversion of (3*R*)-3,4-dihydroxy-2-oxobutanoate (DHOB) to 4-hydroxy-L-threonine (4HT). Red, promiscuous reactions; black, native reactions.

1 mM serine was added the TMM plates to compensate for loss of SerA's normal function in serine synthesis from the deletion of *serA* in *A. fischeri, Af1,* and *Af2.* **Figure 5** shows growth

of Δ*serA Af1*, Δ*serA Af2*, Δ*serA* wild-type *A. fischeri,* and a wild-type *A. fischeri* control on TMM plates with and without supplementation with 10 µM pyridoxine. The lack of growth of Δ*serA Af1* and Δ*serA Af2* on TMM + serine plates and robust growth on TMM + serine + pyridoxine plates suggests that SerA is required for PLP synthesis in the evolved strains.

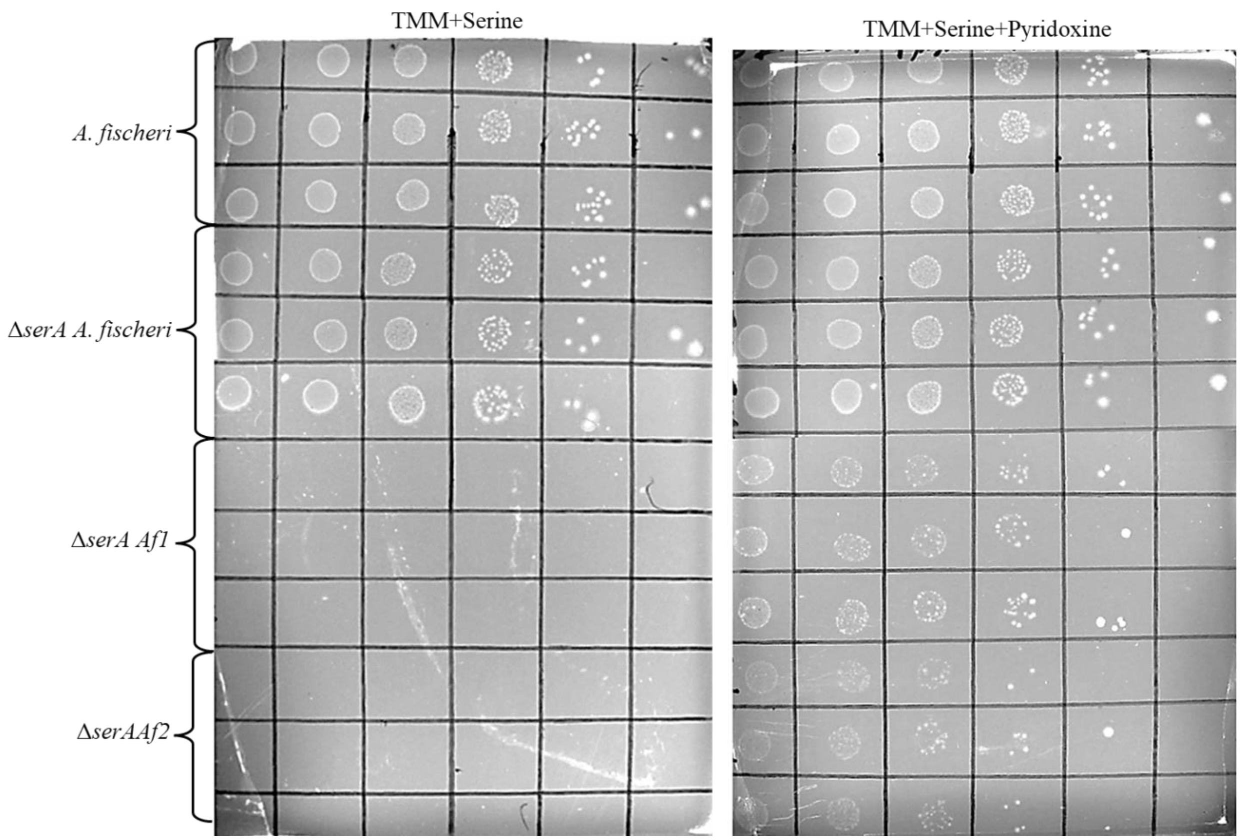

Figure 5. SerA is essential for PLP synthesis in the *Af1* and *Af2* strains. Cultures were prepared as described in Chapter V. 5 µl of diluted cultures were dropped onto the plate and incubated at 28°C for 5 days prior to imaging. Strains were plated in technical triplicate on TMM containing serine (1 mM) in the absence (left) and presence (right) of pyridoxine (10 µM). The wild-type *A. fischeri* positive control ensures that the plates support growth of *A. fischeri.* The growth of the Δ*serA A. fischeri* strain confirms that the amount of serine in the plates compensates for loss of SerA's normal function in serine synthesis. Images are one of three biological replicates.

SerA could contribute through PP1 (**Figure 4**), perform an alternative role in a different protopathway, or replace PdxB in the canonical PLP synthesis pathway. I confirmed the postulated role of SerA in PP1' (**Figure 4**) in *Af1* and *Af2* using kinetic assays. I purified the wild-type SerA and each of the variant SerA enzymes and assayed their activity on the native substrate (3PG) and two possible promiscuous substrates (erythronate and 4PE) (**Table 3**). I also tested inhibition by serine because SerA is normally feedback inhibited by serine (**Figure 6**), because it is the first enzyme in the serine synthesis pathway. 4PE is the native substrate for PdxB. Because SerA and PdxB are homologs that have diverged from a common ancestor, SerA might have some residual PdxB activity and thus be able to directly replace PdxB. This possibility can be eliminated; *A. fischeri* SerA enzymes have no measurable activity with 4PE. However, the *A. fischeri* SerA enzymes had robust activity with erythronate (the promiscuous substrate of SerA in PP1) (**Table 3**), confirming SerA's involvement in PP1. Serine inhibition tests confirmed *A. fischeri* SerA is inhibited by serine (**Figure 6).** Serine inhibition was targeted during evolution in *Af7* because the SerA variant with the V330E amino acid change and decreased inhibition by serine (**Figure 6**).

Table 3. Wild-type and variant *A. fischeri* SerA enzyme k_{cat}/K_M values show amino acid changes in SerA increase k_{cat}/K_M of SerA on erythronate. ND, no delectable activity was observed; NA, insufficient enzyme added. Enzyme assays were measured as described in Chapter III and Chapter V.

SerA enzyme/mutation	k_{cat}/K_{M}, 3PG $M^{-1}s^{-1}$	k_{cat}/K_{M}, erythronate $M^{-1}s^{-1}$	k_{cat}/K_{M}, 4PE $M^{-1}s^{-1}$
***A. fischeri* WT**	1,300 ± 540	0.49 ± 0.25	ND
***A. fischeri* L19F**	NA	0.81 ± 0.22	ND
***A. fischeri* C23Y**	350 ± 71	1.1 ± 0.44	ND
***A. fischeri* S296A**	89 ± 30	2.2 ± 0.88	ND
***A. fischeri* V330E**	370 ± 70	7.6 ± 3.1	ND

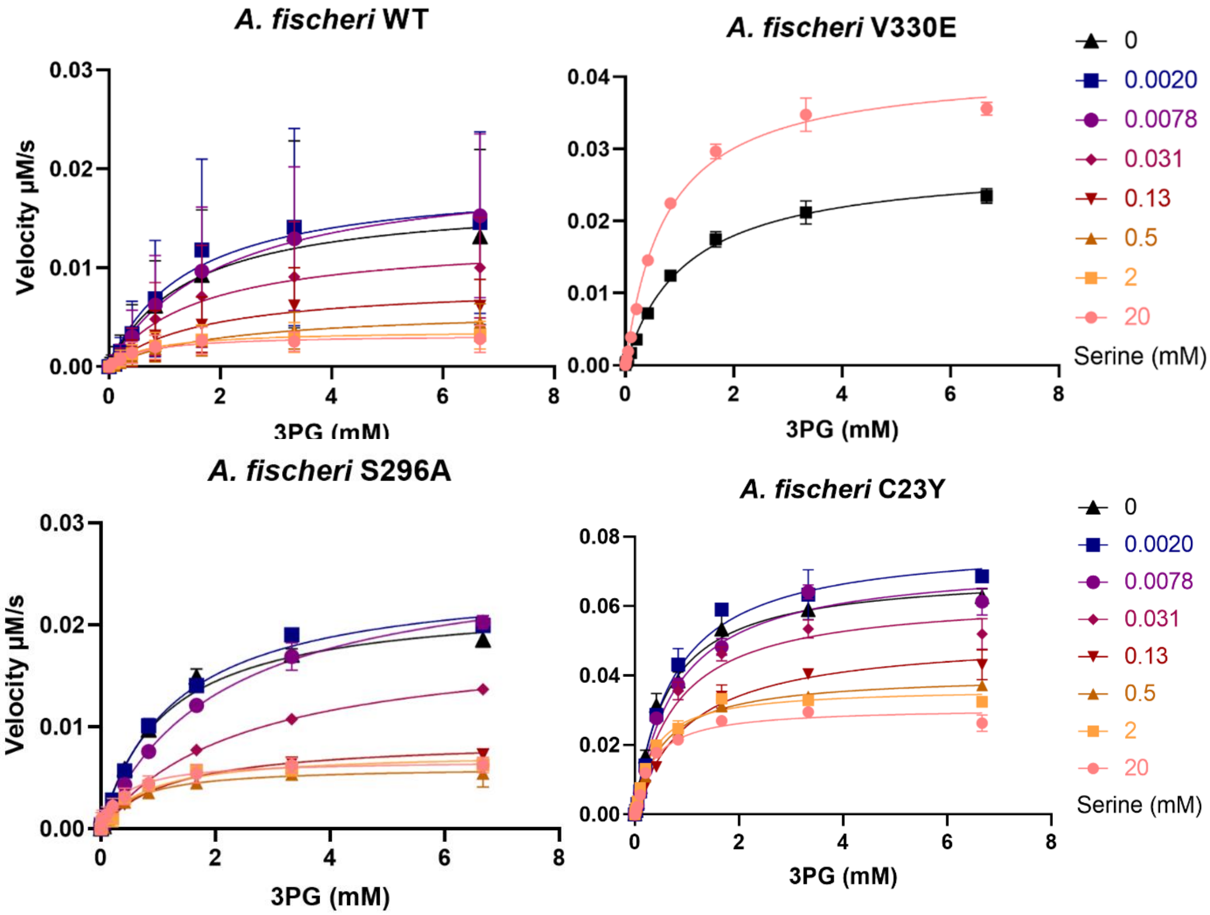

Figure 6. ***A. fischeri*** **SerA with amino acid change V330E decreases inhibition by serine**.

Deletion of *thrB* in the evolved clones and in the wild-type impaired threonine biosynthesis as expected. Threonine (0.4 mM) was added to the TMM to restore growth caused by loss of ThrB's normal function. The lack of growth of *Af1* and *Af2* on TMM + threonine plates and robust growth on TMM + threonine + pyridoxine plates indicates that ThrB involved in PLP synthesis in *Af1* and *Af2* (**Figure 7**). However, there is some growth of *Af1* on TMM plates lacking pyridoxine in the highest concentrated spot dilutions. This could indicate that *Af1* has an alternative route for PLP synthesis or that a different kinase can perform the same reaction as ThrB in PP1. The essentiality of ThrB for PLP synthesis supports its proposed role in PP1 in *Af2* and likely *Af1*.

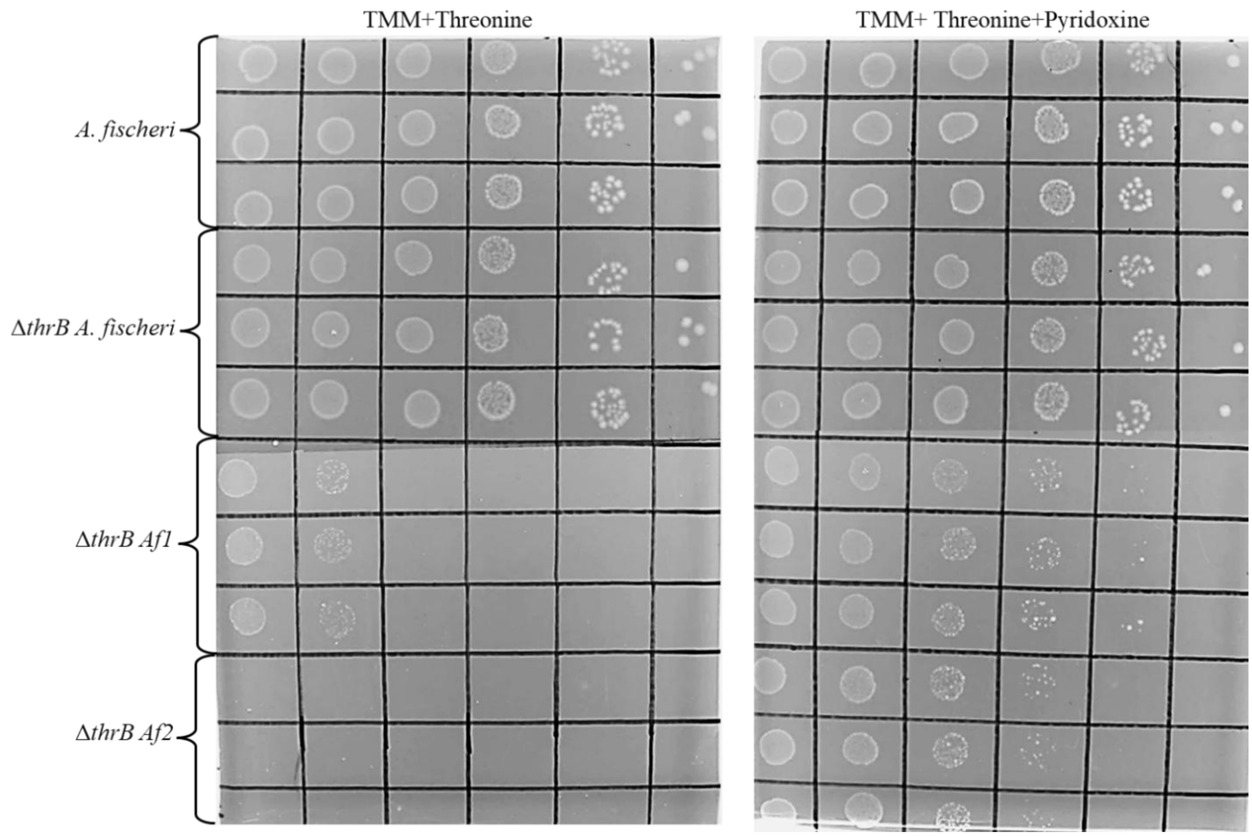

Figure 7. ThrB is essential for PLP synthesis in *Af2* and is involved in *Af1*. Cultures were prepared as described in Chapter V. 5 µl of diluted cultures were dropped onto the plate and incubated at 28°C for 5 days prior to imaging. Strains were plated in technical triplicate on TMM containing threonine (0.4 mM) in the absence (left) and presence (right) of pyridoxine (10 µM). The wild-type *A. fischeri* positive control ensures that the plates support growth of *A. fischeri.* The growth of the Δ*thrB A. fischeri* strain confirms that the amount of threonine in the plates compensates for loss of ThrB's normal function in threonine synthesis. Images are one of three biological replicates.

I performed kinetic assays on ThrB using the native substrate (homoserine) and the proposed promiscuous substrate (4HT) (**Figure 8**). The results of the kinetic assays are shown in **Table 4**.

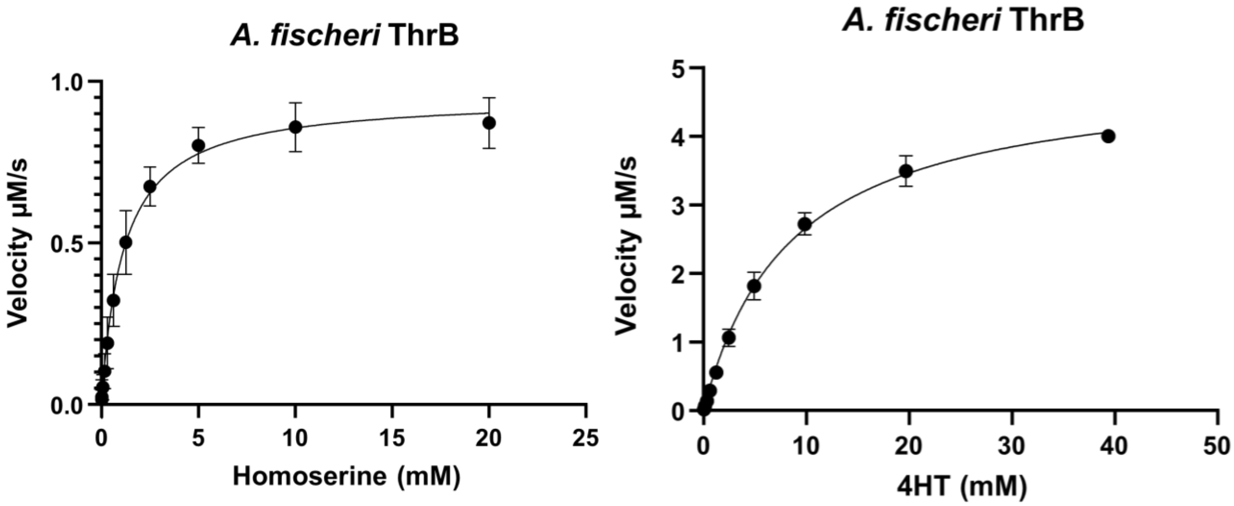

Figure 8. Comparison between *A. fischeri* ThrB enzyme activity on homoserine and 4HT. Enzyme concentration and K_M, k_{cat}, V_{max}, and k_{cat}/K_M values for each assay are listed in **Table 3**. Error bars represent one standard deviation for three technical replicates.

Table 4. Kinetic assays reveal *A. fischeri* ThrB has robust activity on promiscuous substrate in PP1 (4HT). ThrB assays were conducted as described in Chapter V. Enzyme concentration represent the amount of enzyme used in the reaction for the assay.

Substrate	Enzyme (µM)	K_M mM	k_{cat} s^{-1}	V_{max} µM/s	k_{cat}/K_M $M^{-1}s^{-1}$
homoserine	0.025	1.1	38	0.95	3.5×10^4
4HT	0.25	8.5	20	4.94	2.4×10^3

SerC in *A. fischeri* is normally involved in serine biosynthesis and thus deletion of *serA* should impair serine biosynthesis. However, supplementation with serine to rescue growth in TMM in Δ*serC Af1* and *Af2* strains would prevent growth due to the inhibition of SerA, which contributes to PLP synthesis via PP1 in these strains. To avoid this problem, I supplemented the medium with glycine, which can be converted to serine in the cells, providing enough serine for growth without excessively inhibiting SerA. Supplementation with just glycine did not restore the growth of Δ*serC A. fischeri*. I performed a series of additional amino acid supplementation tests, described in Chapter V, and determined that cysteine and tryptophan, which are synthesized from serine in *A. fischeri*, are necessary in addition to glycine. Δ*serC A. fischeri*. Δ*serC Af1*, and Δ*serC Af2* grow poorly on TMM + glycine + cysteine + tryptophan compared to on plates containing the same supplements plus pyridoxine (**Figure 9**). In contrast to the results seen after deletion of *serA* and *thrB* in these strains (**Figures 5 and 7**), deletion of *serC* slows but does not abolish growth. These results indicate that SerC is involved but not required for PLP synthesis in *Af1* and *Af2* (**Figure 9**). There could be an additional aminotransferase involved in the *Af1* and *Af2* PP1 pathway, or a different protopathway requiring SerA and ThrB and not SerC. The reduction in growth of the Δ*serC A. fischeri* strain which had not evolved PP1 indicated an alternative aminotransferase could also perform the SerC reaction in the canonical PLP synthesis pathway.

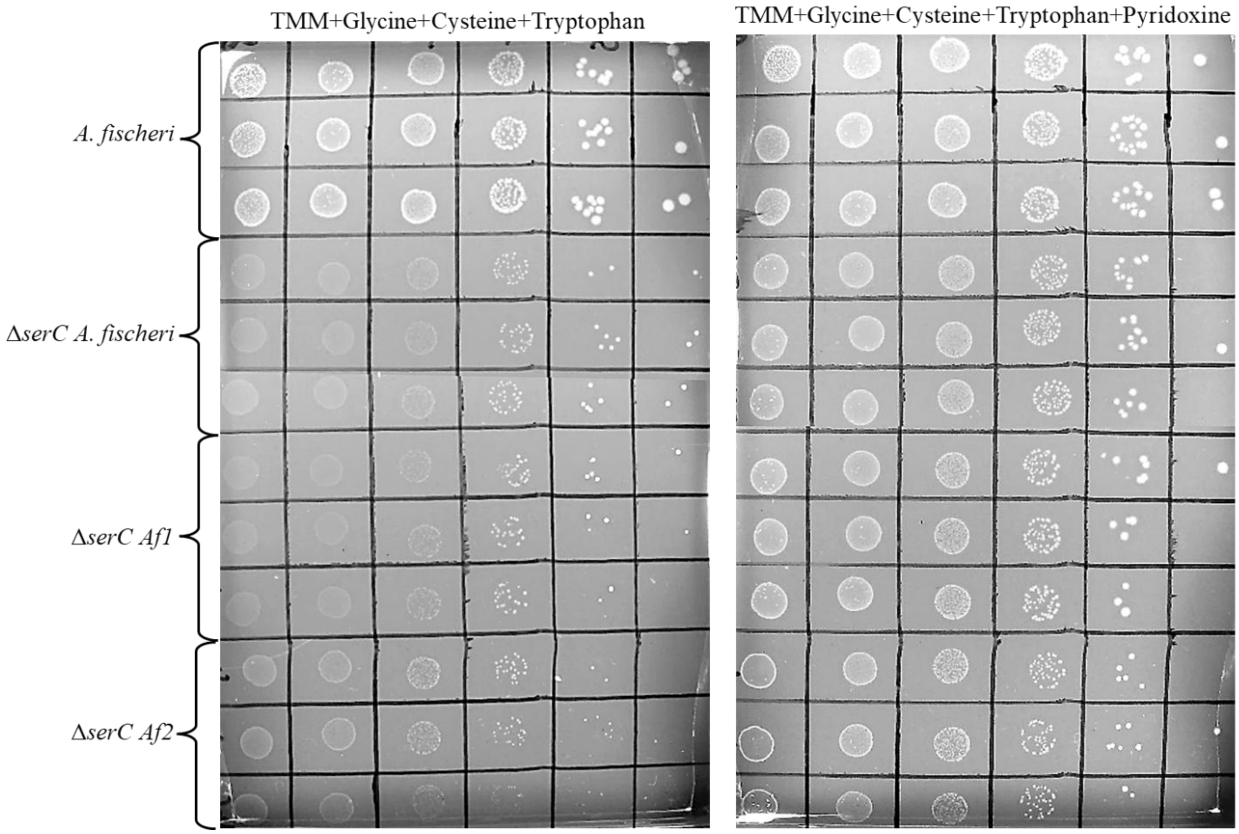

Figure 9. SerC contributes to PLP synthesis in *Af1* and *Af2*. Cultures were prepared as described in Chapter V. 5 µl of diluted cultures were dropped onto the plate and incubated at 28°C for 5 days prior to imaging. Strains were plated in technical triplicate on TMM containing glycine (10 mM), cysteine (0.2 mM), and tryptophan (0.1 mM) in the absence (left) and presence (right) of pyridoxine (10 µM). The wild-type *A. fischeri* positive control ensures that the plates support growth of *A. fischeri.* The growth of the Δ*serC A. fischeri* strain confirms that the concentration and number of amino acids in the plates compensates for loss of SerC's normal function in serine synthesis. Images are one of three biological replicates.

The possibility that an alternative aminotransferase can catalyze the conversion of DHOB to 4HT in these strains is plausible because aminotransferases are highly expressed in minimal medium to synthesize necessary amino acids and often have broad substrate specificity. *E. coli* has over 22 annotated aminotransferases (Berglund et al. 2012; Peña-Soler et al. 2014; Koper et al. 2022), and *A. fischeri* probably has a similar number. The AspC aminotransferase appeared as a likely candidate to perform the SerC reactions in PP1 because it has broad specificity with over seven known substrates, and multiple of which are bulky or have negatively charged groups (**Figure 10**) (Koper et al. 2022). AspC has multiple positively charged groups in the active site, which could facilitate binding of the promiscuous substrate in PP1 (DHOB). Currently AspC has not been tested for activity with DHOB.

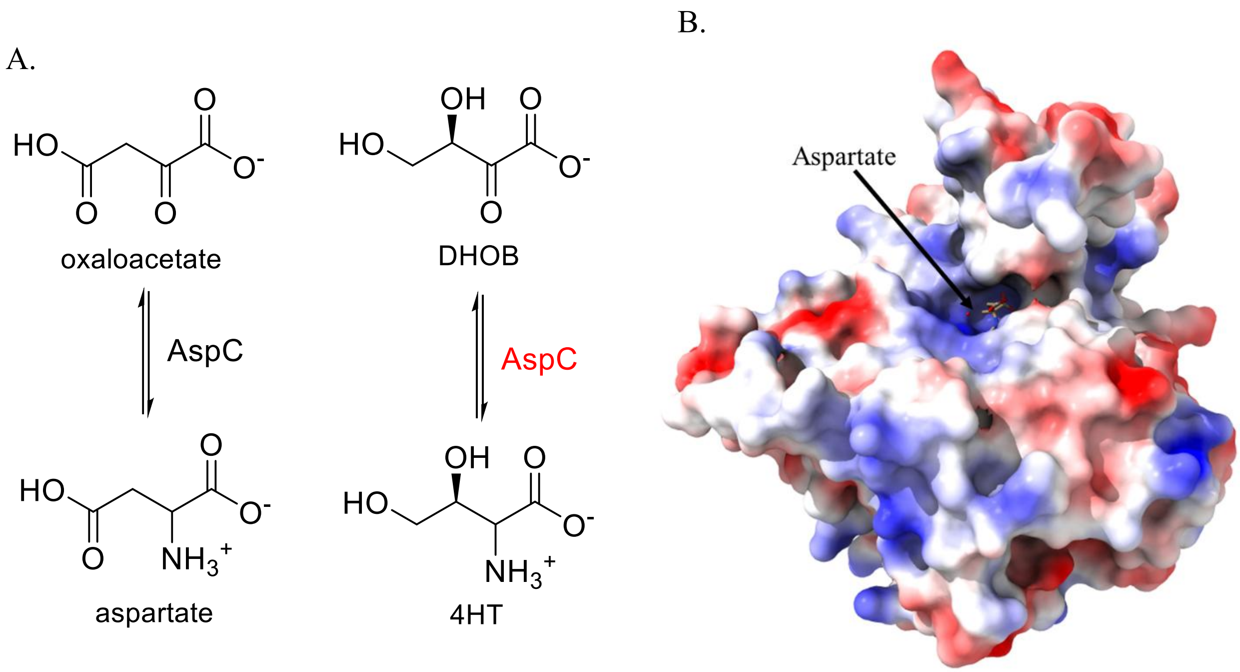

Figure 10. AspC could catalyze the promiscuous reaction in PP1. A. AspC's native reaction (left) is similar to the promiscuous reaction in PP1 (right). B. AspC structure (Q5E4R3) created by SWISS-UniProt from an AlphaFold1 predicted structure and displayed in ChimeraX (Pettersen et al. 2021; The UniProt Consortium 2025). Blue represents positively charged residues and red represents negatively charged residues. Enzyme is modeled with aspartate in active site.

I deleted *aspC* in wild-type *A. fischeri* and the *Af1* and *Af2* strains to test whether it is involved in PLP synthesis. *aspC* is essential for growth in *A. fischeri*; Δ*aspC A. fischeri* is unable to grow on TMM plates. I performed amino acid supplementation tests (described in Chapter II) and found that a combination of aspartic acid, tyrosine, and phenylalanine was required to restore growth due to the loss of AspC's native function. I was not able to achieve full restoration of growth. However, the strains grew sufficiently well for visual analysis of the importance of AspC for PLP synthesis. The growth tests showed a reduction in growth of Δ*aspC Af1* and Δ*aspC Af2* on TMM plates lacking pyridoxine compared to Δ*aspC A. fischeri*. Addition of pyridoxine slightly improved growth (**Figure 11**), most clearly in the *Af2* strain (**Figure 11**), indicating that AspC is more important for PLP synthesis in *Af2* than *Af1*. Future kinetic assays of AspC will be necessary to confirm that AspC can catalyze the proposed conversion of DHOB to 4HT.

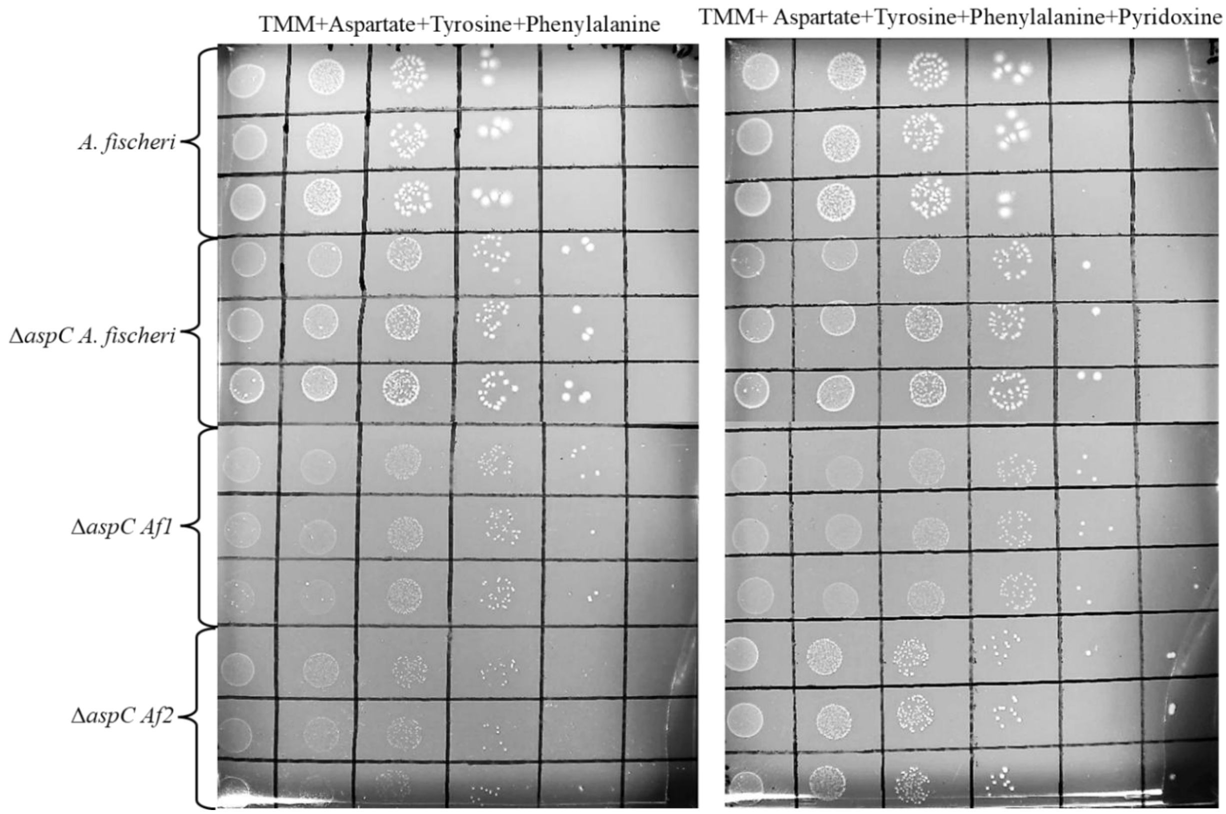

Figure 11. AspC contributes to PLP synthesis in *Af1* and *Af2*. Cultures were prepared as described in Chapter V. 5 µl of diluted cultures were dropped onto the plate and incubated at 28°C for 5 days prior to imaging. Strains were plated in technical triplicate on TMM containing glycine (10 mM), aspartate (4 mM), phenylalanine (0.04 mM), and tyrosine (0.02 mM) in the absence (left) and presence (right) of pyridoxine (10 µM). The wild-type *A. fischeri* positive control ensures that the plates support growth of *A. fischeri.* The growth of the Δ*aspC A. fischeri* strain confirms that the concentration and number of amino acids in the plates compensates for loss of AspC's normal function in aspartate synthesis. Images are one of three biological replicates

The growth of evolved strains lacking genes required for PP1 and the kinetic assays of SerA and ThrB are consistent with the operation of PP1 (**Figure 4**) in *Af1* and *Af2*. Both SerC and AspC enzymes are likely involved in PLP synthesis, with SerC contributing more than AspC. AspC may also contribute more in *Af2* than in *Af1*. The involved genes suggest that a version of PP1 restored PLP synthesis in *Af2*. The version of PP1 is annotated as PP1' to indicate the utilization of AspC in addition to SerC to catalyze the transamination rection of DHOP to 4HT.

The essentiality of SerA and the involvement of ThrB, SerC, and AspC suggest that *Af1* evolved the same PP1' pathway as *Af2*. However, the partial requirement of ThrB is still unclear. It is still unclear whether *Af1* can use an additional route to synthesize PLP in addition to PP1'.

Mutations in *yidA* and *serA* helped restore PLP synthesis during evolution of *A. fischeri* Δ*pdxB*

Mutations in *serA* and *yidA* appeared to be important for the evolution of PP1', with all lineages acquiring mutations in both genes after the fifth passage (**Table 1**). YidA and SerA could have significant effects on flux into and through the PLP synthesis pathway, allowing the evolved strains to synthesize more PLP. Mechanisms by which mutations in *yidA* and *serA* might help restore PLP synthesis are described below.

Mutations in yidA could increase flux into PLP synthesis

Mutations in *yidA* arose in six of the eight evolved lineages of Δ*pdxB A. fischeri* (**Table 1**). Two mutations introduced an early stop codon and one resulted in a 44 amino acid deletion that likely cause loss of function of the enzyme. The other mutations were a one amino acid deletion and non-synonymous amino acid changes. YidA is a broad-specificity sugar phosphatase (Kuznetsova et al. 2006). The precursor of 4PE in the PLP synthesis pathway is erythrose-4-

phosphate (E4P) (**Figure 4**). YidA has high activity with E4P, converting it to erythrose (k_{cat}/K_M = 1.0 x 10^6 $M^{-1}s^{-1}$) (Kuznetsova et al. 2006), and shunting E4P away from PLP synthesis. Loss of function mutations in YidA could increase the concentration of E4P, thereby increasing flux into PLP synthesis.

Mutations in serA contributed to PLP synthesis in ΔpdxB A. fischeri strains

Six out of the eight independently evolved strains acquired mutations in *serA*, with *serA* mutations present in all strains isolated at the end of the fifth passage. Two of the mutations were identical. The residues impacted by the mutations are coloured in the predicted *A. fischeri* SerA structure below (**Figure 12**). All *serA* mutations seen in the *A. fischeri* evolution are near the active site, with one mutation V330E located in the serine binding region of the allosteric regulatory site (**Figure 12**).

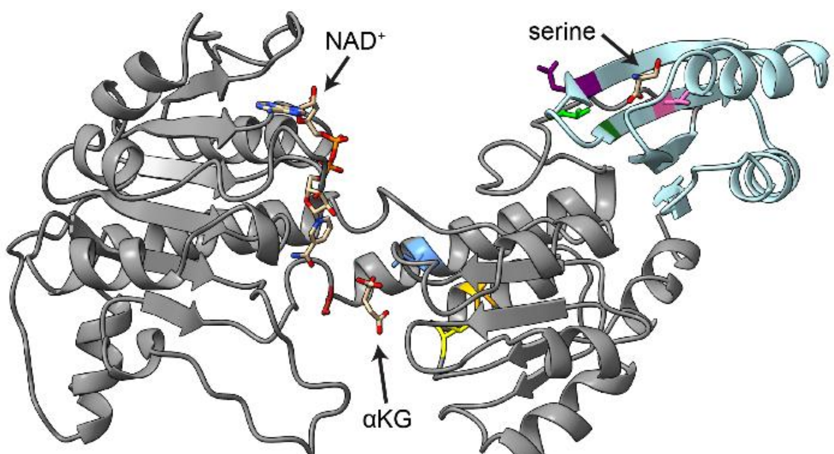

A. fischeri	
residue	amino acid change
Leu19	Leu → Phe
Cys23	Cys → Tyr
Ser296	Ser → Ala
Gln330	Gln → Pro

E. coli	
residue	amino acid change
Ile381	+Met-Val
Ile340	Ile → Leu
Gln371	Gln → Pro
Gly377	Gly → Cys

Figure 12. **Amino acid changes in SerA are located in the active site and regulatory region.** Mutated residues in evolved *A. fischeri* Δ*pdxB* and *E. coli* Δ*pdxB* listed in the tables correspond to colours mapped to the predicted structure of *A. fischeri* SerA. The SerA structure was predicted using AlphaFold3 with NAD^+ bound with α-ketoglutarate (αKG), which is similar to 4PE, in the active site (Abramson et al. 2024). Created by Dr. Widney (Widney 2024).

Kinetic assays of the *A. fischeri* SerA wild-type and mutant enzymes revealed that all mutations increased the k_{cat}/K_M for erythronate (**Table 3**). Thus, the mutations allowed SerA to better catalyze the conversion of erythronate to DHOB in PP1'. The V330E mutation decreased allosteric inhibition by serine (**Figure 6**), allowing the SerA enzyme to be more active and able to participate in the PP1' pathway. Additionally, the mutation in the promoter region of *serA* in *Af8* may have increased expression of L19F SerA in this strain.

Discussion

Δ*pdxB A. fischeri* overcame the deletion of *pdxB* by evolving PP1'. This protopathway restored PLP synthesis by shunting 4PE away from the canonical PLP synthesis pathway upstream of PdxB into the PP1' pathway and generating 4PHT downstream of the *pdxB* deletion, and SerC (**Figure 4**). The PP1' pathway that evolved in *A. fischeri* Δ*pdxB* is similar to PP1 in evolved strains of Δ*pdxB E. coli*. However, the mutations that arose in the two species are very different. *E. coli* acquired more mutations and took longer to evolve than *A. fischeri*. This finding suggests that PP1' evolves more easily in *A. fischeri* than PP1 in *E. coli*, possibly because *A. fischeri* SerA is more efficient at catalyzing the reaction of erythronate to DHOB. Additionally, *A. fischeri* SerA could be less inhibited by serine than *E. coli* SerA, rendering the SerA enzyme more available to participate in both an evolved PLP synthesis pathway and its canonical serine synthesis pathway. These possibilities are further described in Chapter IV.

Chapter III

Differences between the promiscuous activities of 3-phosphoglycerate dehydrogenase orthologs and their influence on bacterial evolution after deletion of *pdxB*

Introduction

E. coli was subjected to the evolutionary challenge of restoring PLP synthesis after the deletion of pdxB. One isolated clone in an evolved Δ*pdxB* strain revealed PP1 evolved to restore PLP synthesis. Four bacteria *Aliivibrio fischeri*, *Pseudomonas putida*, *Salmonella enterica*, and *Acinetobacter baylyi* were subject to the same evolutionary challenge. Dr. Karl Widney deleted *pdxB* in *A. fischeri, P. putida* and *S. enterica* and conducted laboratory evolution of the strains in the appropriate minimal medium for each organism (Widney 2024). Dr. Della Fixsen deleted *pdxB* in *Acinetobacter baylyi* and found *A. baylyi* can restore PLP synthesis without evolution. Amongst the majority of evolved Δ*pdxB* bacteria, SerA is required for PLP synthesis shown by genetic evidence (**Table 5**). Genetic evidence determines the genes essential for PLP synthesis in Δ*pdxB* evolved strains. I carried out the genetic experiments in evolved strains of Δ*pdxB A. fischeri.* Genetic experiments in evolved strains of Δ*pdxB S. enterica* and *P. putida* were performed by post-docs Dr. Dong-Dong Yang and Dr. Della Fixsen and technician Daniel Yoshimura

Table 5. **Genes essential for PLP synthesis in evolved Δ*pdxB* strains.** Genes predicted to be involved in PLP synthesis restoration in evolved Δ*pdxB* strains were deleted. Colours depict the effect of the gene deletion on growth relative to growth with 10 μM pyridoxine. Black, abolished growth; grey, reduced growth; green, unaffected growth; white, untested. ***, mutation in that gene was found in the corresponding strain.

	E. coli	***P. putida***	***A. fischeri***		***S. enterica***		
	Ec1	*Pp1*	*Af1*	*Af2*	*Se1a*	*Se2b*	*Se3*
Δ*serA*			***				
Δ*thrB*							
Δ*serC*							
Δ*aspC*							
Δ*pdxA*							
Δ*glyA*							
Δ*nudL*							
Δ*ltaE/ltaA*							
Δ*pdxA-2*					***		
Δ*dtnK*							
Δ*yigB*							***
Δ*dtnR*						***	
Δ*thrB* Δ*dtnK*							

SerA could contribute to PLP synthesis in the evolved Δ*pdxB* bacteria in multiple ways. SerA can catalyze the oxidation of erythronate to DHOB in *E. coli* PP1, as shown by Kim et al., and in *A. fischeri* PP1', as described in Chapter II. SerA might also perform the native function of PdxB converting 4PE to HOPB. SerA and PdxB are evolutionarily related and are structurally similar. Additionally, they catalyze similar reactions (**Figure 13 and 14**). Genetic evidence in evolved Δ*pdxB P. putida* strains gathered by Daniel Yoshimura and in unevolved Δ*pdxB A. baylyi* gathered from Dr. Della Fixsen suggests that SerA replaced PdxB for PLP synthesis. Finally, Dr. Yang and Dr. Fixsen have shown that evolved *S. enterica* Δ*pdxB* strains can restore PLP synthesis via three different routes, two of which involve SerA. The goal of the work described in this chapter was to determine whether variations in the promiscuous activities of SerA influence the route by which PLP synthesis is restored. I purified and assayed twenty wild-type and mutant SerA enzymes from five different bacteria in an effort to correlate levels of promiscuous activities with either the emergence of a protopathway or the direct replacement of PdxB by SerA.

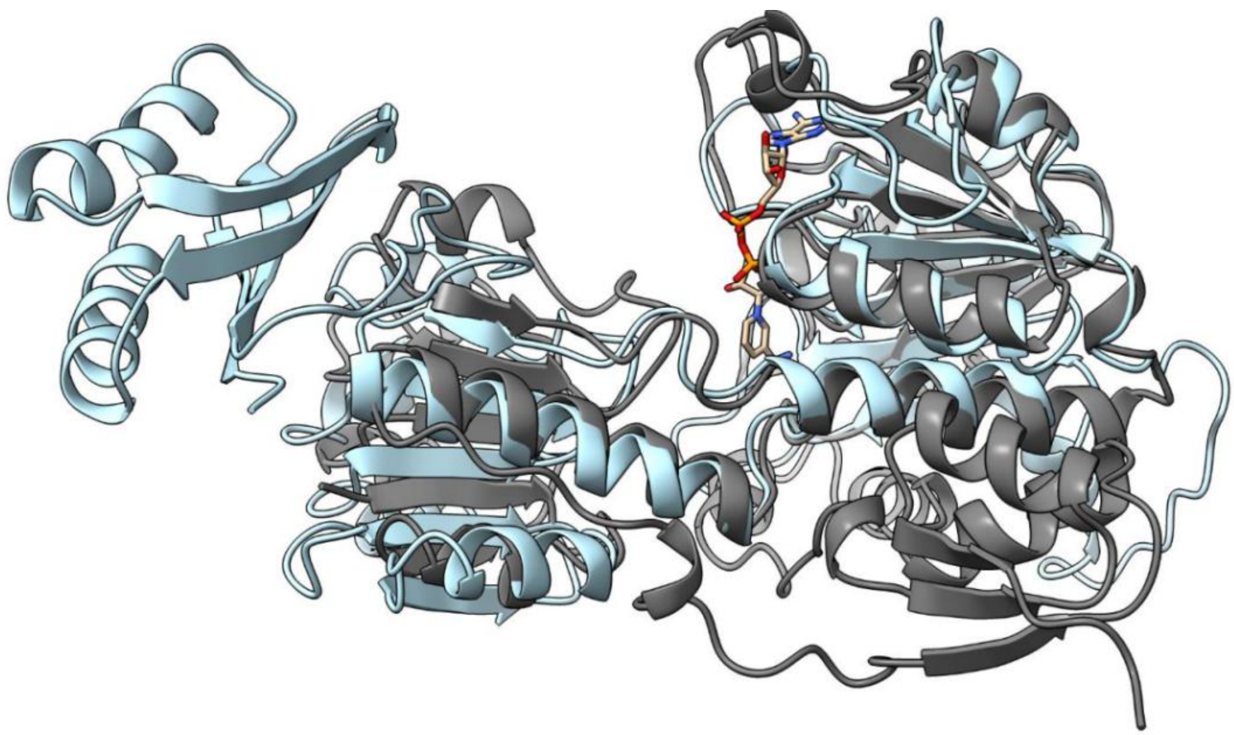

Figure 13. SerA and PdxB are structurally similar. Grey, SerA; Blue, PdxB. Model displayed in Chimera X and created using Matchmaker (Pettersen et al. 2021). The crystal structure of *E. coli* SerA is bound to NAD^+ and serine (Schuller et al., 1995). *E. coli* PdxB structure was predicted using AlphaFold 3 (Abramson et al. 2024). Created by Dr. Widney (Widney 2024).

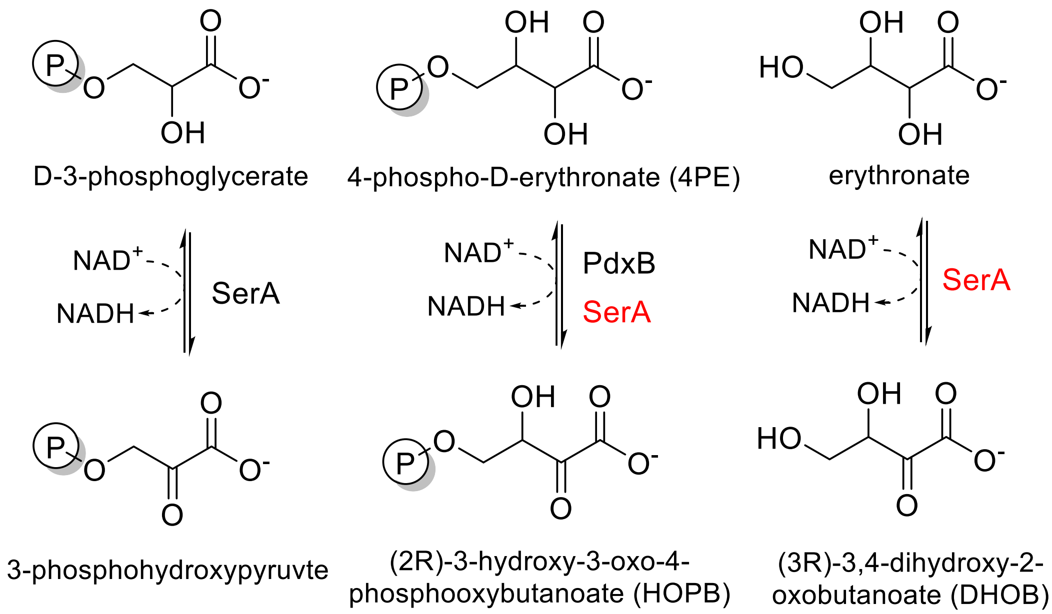

Figure 14. **The reactions catalyzed by SerA and PdxB are similar.** Black, native reactions; red, promiscuous reactions

SerA kinetic assay scheme

SerA kinetic assays were performed using the coupled reaction shown in **Figure 15** (described in detail in Chapter V). This assay was used by former post-doc Dr. Juhan Kim in the initial characterization of PP1 in evolved strains of Δ*pdxB E. coli* (Kim et al. 2019). It is complex because the native and promiscuous SerA reactions are energetically unfavorable (Zhang et al. 2017). Zhang et al. 2017 discovered that the rate of the native reaction can be measured by coupling the reaction to the energetically favorable reaction of 2-ketoglutarate (2KG) to 2-hydroxyglutarate (2HG). SerA couples the two reactions through the interconversion between NAD^+ and NADH (Zhang et al. 2017). NAD^+ is used as the cofactor for 3PG dehydrogenation. The NADH product remains attached to SerA because of its extremely tight binding to the enzyme. This then allows SerA to use the bound NADH in the favorable reaction of 2KG to 2HG. Thus, SerA continuously recycles the NAD cofactor on the enzyme. The coupling of 2KG to 2HG occurs naturally in vivo to facilitate the dehydrogenation of 3PG (Zhang et al. 2017). The product 2HG is converted back to 2KG by the enzyme D-2HG dehydrogenase (D2HGDH) (Zhang et al. 2017).

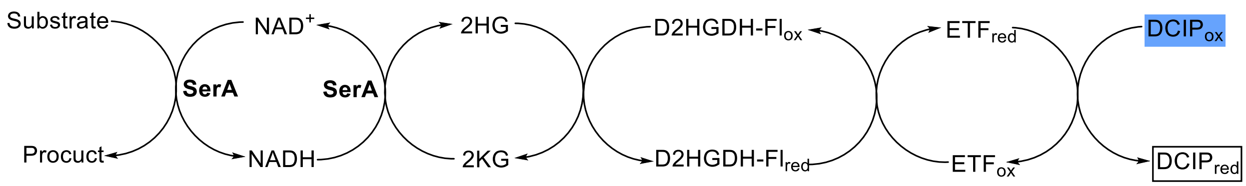

Figure 15. Coupled assay scheme used to measure the catalytic activity of SerA enzymes. SerA catalyzes the conversion of the substrate and the reaction is coupled to the conversion of 2-ketoglutarate (2KG) to 2-hydroxyglutarate (2HG) by recycling NADH on the enzyme. The 2KG is regenerated by the reduction and oxidation of the enzyme D-2hydroxyglutarate dehydrogenase (D2HGDH). The conversion between the oxidized and reduced forms are coupled to the electron-transferring flavoprotein A and B (ETFAB) and coupled to the reduction of 2,6-Dichlorophenolindophenol (DCIP). The oxidized form of DCIP is blue, allowing the change in absorbance to reflect SerA activity.

Many kinetic assays of SerA measured activity through the absorbance readout of the reduction of NAD^+ to NADH (Zhao and Winkler 1996). However, when 3PG is used as the substrate no more than one turnover can occur without the presence of 2KG, preventing the ability to measure the maximum activity of SerA on 3PG dehydrogenation in vitro. Further, because NADH is recycled on the SerA enzyme during the coupled reaction, the activity cannot be measured through the change in absorbance of NAD^+. Coupling the SerA reaction to the 2HGDH reaction in conjunction with the coupling enzyme ETFAB allows electron transfer to DCIP. Thus, measuring the rate of reduction of DCIP in the coupled reaction directly correlates to the rate of dehydrogenation of 3PG. I used this coupled assay to measure both the native and promiscuous activities of SerA.

Enzymatic activities of SerA enzymes vary across species

The catalytic activities of SerA enzymes varied significantly between species and were affected by the mutations in *serA* (**Table 6**). The values for the *E. coli* enzyme agree with the previously published activity of wild-type *E. coli* SerA by Kim et al. 2019 using the same kinetic assay scheme. *E. coli*, *P. putida*, *E. enterica*, and *A. fischeri* SerAs all had robust activity with the native substrate, 3PG. There are striking differences that differ by 10-fold in the promiscuous activities of the five wild-type SerA enzymes from different bacteria. A. fischeri SerA has no detectable activity with 4PE, while E. coli has a k_{cat}/K_M ($M^{-1}s^{-1}$) of ~ 18. Notably, *A. baylyi* and *P. putida* have the highest activity with 4PE, about 10-fold higher then E. coli. All SerA enzymes have activity with erythronate, especially *A. baylyi* that has over 10-fold higher activity than the four other wild-type SerA enzymes.

Table 6. **Catalytic activities of SerA enzymes.** Errors represent one standard deviation. ND, not detectable; NA, insufficient enzyme added. Amino acid changes in blue, residue change located in regulatory region of SerA.

	$k_{cat}/K_{M,\ 3PG}$ ($M^{-1}s^{-1}$)	$k_{cat}/K_{M,\ erythronate}$ ($M^{-1}s^{-1}$)	$k_{cat}/K_{M,\ 4PE}$ ($M^{-1}s^{-1}$)
A. fischeri **WT**	1,300 ± 540	0.49 ± 0.25	ND
A. fischeri **L19F**	NA	0.81 ± 0.22	ND
A. fischeri **C23Y**	350 ± 71	1.1 ± 0.44	ND
A. fischeri **S296A**	89 ± 30	2.2 ± 0.88	ND
A. fischeri **V330E**	370 ± 70	7.6 ± 3.1	ND
P. putida **WT**	6,800 ± 1200	2.4 ± 0.36	170 ± 23
S. enterica **WT**	2,700 ± 480	1.4 ± 0.40	79 ± 6.5
A. baylyi **WT**	660 ± 100	35 ± 0.56	860 ± 200
E. coli **WT**	5,200 ± 860	0.19 ± 0.37	18 ± 0.51
E. coli **V16G**	37 ± 200	0.78 ± 0.15	24 ± 1.5
E. coli **+403G**	780 ± 260	29 ± 9.7	300 ± 83
E. coli **S296A**	84 ± 25	0.28 ± 0.1	7.0 ± 0.74
E. coli **+381MV**	550 ± 130	0.22 ± 0.25	33 ± 3.1
E. coli **I304L**	1,400 ± 460	0.52 ± 0.10	140 ± 66
E. coli **L47S**	1,300 ± 270	186 ± 70	210 ± 4.6
E. coli **Q370P ΔT371**	1,800 ± 440	0.31 ± 0.19	41 ± 11
E. coli **T63N**	1,300 ± 350	12 ± 3.3	1,000 ± 420
E. coli **G377C**	1,400 ± 470	130 ± 22	620 ± 320
E. coli **ΔL351**	2,800 ± 380	3 ± 2.8	200 ± 520
E. coli **ΔN355**	3,000 ± 800	2.5 ±0.32	300 ± 170

Promiscuous activities of wild-type SerA enzymes influence the mechanism for restoration of PLP synthesis

Mutations in *serA* arose during evolution of both Δ*pdxB E. coli* and Δ*pdxB A. fischeri*. Δ*pdxB E. coli* acquired *serA* mutations in four out of ten lineages and Δ*pdxB A. fischeri* acquired *serA* mutations in six out of eight lineages (**Table 7**). Clearly mutations in *serA* are beneficial for fitness or PLP synthesis in *E. coli* and *A. fischeri* during evolution. However, mutations in *serA* did not arise in the other Δ*pdxB* organisms (**Table 7**). We hypothesized that understanding the ability of wild-type SerA enzymes to perform promiscuous reactions required for PLP synthesis in Δ*pdxB* bacteria could provide insight into why mutations in *serA* were helpful for Δ*pdxB E. coli* and *A. fischeri*.

Table 7. Mutations acquired during evolution of multiple populations of Δ*pdxB* bacteria Created by Dr. Widney (Widney 2024**).**

	name	population doublings	~ μ (% of WT)	*glyA (II*)*	*yidA*	*serA*	*rpe*	*dtnR*	*ybhA*	*pgl*	*gapA*	*ettA*	*purF*	*rhlB*	*ackA*	*ilvH*	*rpoS*	*nadR*	*pykF*	*rng*	*gltB*
P. putida	*Ppjc1*	20	69	N																	
	Ppjc2	21	69	N																	
	Pp1	18	75	N																	
	Pp2	17	75	N																	
A. fischeri	*Af1*	15	27			N															
	Af2	14	29		E																
	Af3	13	25		L																
	Af4	15	31			N															
	Af5	36	38		N	N															
	Af6	34	30		E	N															
	Af7	34	30		I	N															
	Af8	35	36		N	N, X															
S. enterica	*Se1a*	44	30																		
	Se1b	44	30	I	F																
	Se2a	36	40											F	L						
	Se2b	36	40					N						F	L						
	Se3	46	33				L														
	Se4	20	33					L													
	Se5	38	35					F													
	Se6	41	33					F													
E. coli	*Ec1*	151	48						L	L	N						F				
	Ec2	149	55						L	L	N	I	N								L
	Ec3	131	66						L	L	N					N				N	
	Ec4	143	50				L		F												
	Ec5	162	34						L	L	N	L	N			N		L			
	Ec6	141	52			I					N	N									
	Ec7a	130	64						L	L	N		N				N	F			
	Ec7b	130	53			N			L	L	N								F		
	Ec8	139	74			N, D					N	N									F
	Ec9	124	69			N			L	L	N								I		
	Ec10	110	29				F		N		N					N				I	

N, nonsynonymous; F, small (<10 bp) frameshift insertion or deletion; I, small (< 10 bp) in-frame insertion or deletion; L, large ≥ 10 bp insertion or deletion; X, intergenic; E, early stop codon. *, *glyA-II* found only in *P. putida*.

Mutations in serA increase SerA promiscuous activity with erythronate or 4PE

Amino acid changes in *A. fischeri* SerA caused by mutations in *serA* increased activity of SerA with erythronate (**Table 6**); amino acid changes in *E. coli* SerA caused by mutations in *serA* increased activity of *E. coli* SerA with erythronate, 4PE, or both. The higher activity with erythronate of *A. fischeri* SerA variants in Δ*pdxB* strains allows SerA to better participate in PP1'. Increased activity on erythronate of *E. coli* SerA variants allows SerA to better participate in PP1 in Δ*pdxB* strains. Additionally, amino acid changes in *E. coli* SerA that increased activity on 4PE nearly 50-fold could enable the replacement of PdxB's activity with SerA. The replacement of PdxB by SerA in those strains still needs to be confirmed through genetic evidence.

Some mutations in serA affect feedback inhibition of SerA by serine

SerA is the first enzyme in the serine synthesis pathway and is subject to feedback inhibition by serine. This regulation helps the cell conserve resources when serine levels are sufficient. Inhibition of serine in evolved Δ*pdxB* cells that rely on SerA for PLP synthesis would not only diminish serine synthesis, but PLP synthesis as well. Some mutations in *serA* that arose during evolution of *E. coli* Δ*pdxB* and *A. fischeri* Δ*pdxB* affect residues in the regulatory domain of the enzyme, specifically in the serine binding site. These mutations might diminish feedback inhibition by serine to enable SerA to participate more in PLP synthesis.

I tested the inhibition of SerA activity by serine for each of the twenty enzymes listed in **Table 6.** The *A. fischeri* V330E SerA, described in Chapter II, is not inhibited by serine. The amino acid change V330E diminished serine inhibition of *A. fischeri* SerA (**Figure 6**).

Low inhibition by serine was also seen in *A. baylyi* wild-type SerA; serine inhibition was lowered in some *E. coli* mutated SerA enzymes. (**Figure 16**). **Figure 16** shows the wild-type and mutated E. coli SerA enzymes. These mutations in SerA were visually qualified to decrease inhibition by serine and are representative of the other enzymes characterized as having low inhibition.

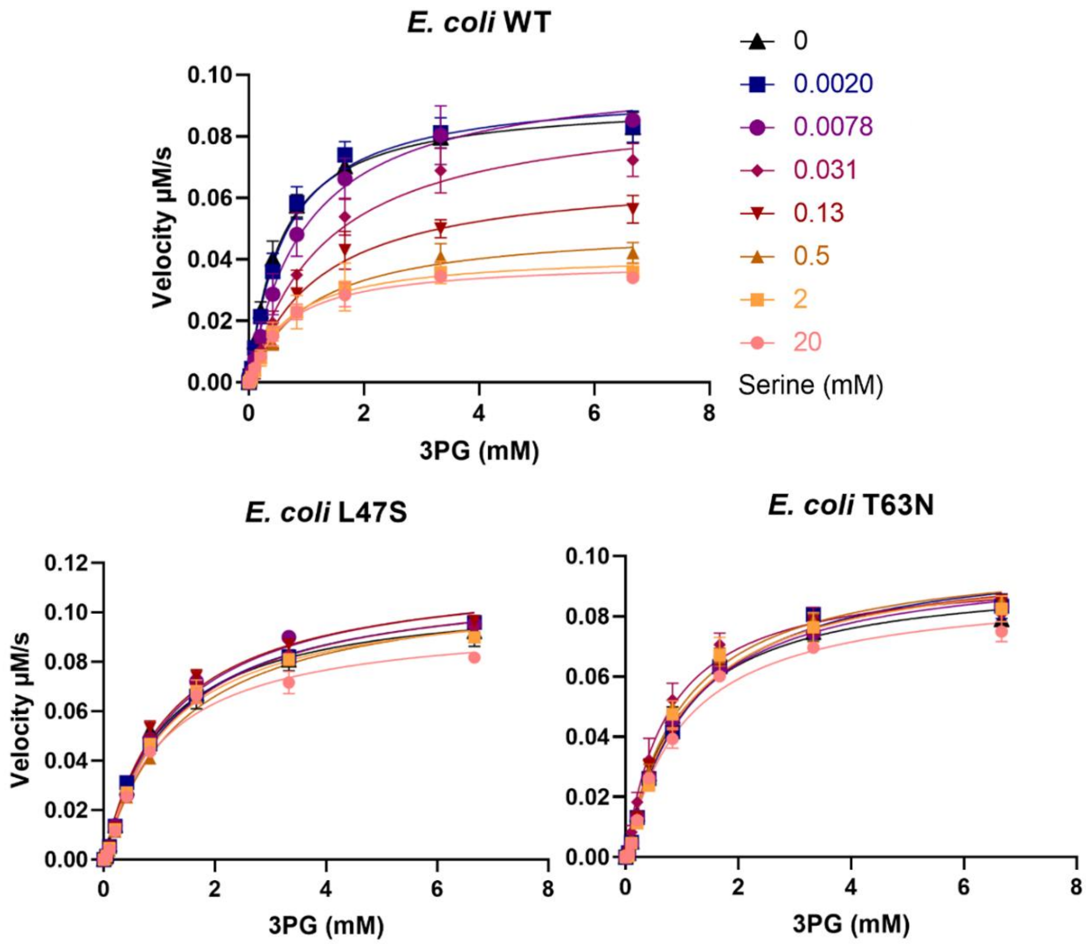

Figure 16. The amino acid changes L47S and T63N in *E. coli serA* decrease inhibition of SerA by serine.

The promiscuous activities of SerA influence the accessibility of various mechanisms for restoration of PLP synthesis after deletion of pdxB

The catalytic activity of SerA enzymes on the promiscuous substrates erythronate and 4PE differ between organisms. *A. baylyi* SerA has an unusually high activity with both erythronate and 4PE. Notably, the 4PE dehydrogenase activity of *A. baylyi* SerA is equivalent to its 3PG dehydrogenase activity. Dr. Fixsen found that deletion of *pdxB* in *A. baylyi* does not comprise growth. Thus, the high promiscuous 4PE dehydrogenase activity of *A. baylyi* SerA appears to be sufficient to replace PdxB.

P. putida and *S. enterica* SerAs have lower but still significant activities with 4PE. Genetic experiments suggest that Δ*pdxB A. fischeri* and Δ*pdxB E. coli* have much lower activity with 4PE. Indeed, I was unable to detect any 4PE dehydrogenase activity in *A. fischeri* SerA. Thus, these bacteria are more likely to restore PLP synthesis by evolving a novel protopathway.

The mutations in *serA* that arose during the evolution of Δ*pdxB E. coli* and *A. fischeri* strains increase PLP synthesis via PP1 or PP1' by increasing SerA's activity with erythronate and in some cases by decreasing feedback inhibition by serine (**Table 6 and Figures 6 and 16**). Interestingly, these mutations decrease the native activity of SerA on 3PG (**Table 6**), potentially compromising serine biosynthesis. Additionally, mutations in *gapA* arose in Δ*pdxB E. coli* which decreased the concentration of serine present in the cells (Kim et al. 2019). However, the tradeoff between improving synthesis of PLP and compromising synthesis of serine is clearly worth it.

Discussion

The activities of orthologous enzymes with both their native and promiscuous substrate can vary significantly (Rix et al. 2020). The patterns of catalytic activities of SerA differed significantly across bacteria and patterns provide insight into how SerA can be recruited to restore PLP synthesis. In *E. coli* and *A. fischeri,* the wild-type SerA promiscuous activities were lower than in *A. baylyi, P. putida*, and *S. enterica*. Every observed mutation in *serA* increased the promiscuous activity on erythronate or 4PE in both *E. coli* and *A. fischeri*.

A. baylyi SerA has the highest activity with 4PE, similar to the activity it has on 3PG, indicating the SerA enzyme may be more promiscuous in nature compared to the other SerA enzymes tested. Additionally, *A. baylyi* SerA is not inhibited by serine. *A. baylyi* Δ*pdxB* grows in minimal medium without evolution, indicating that *pdxB* is not an essential gene. Dr. Fixsen has shown that Δ*pdxB A. baylyi* does require SerA for PLP synthesis. This indicates that SerA can replace the function of PdxB (**Figure 17**).

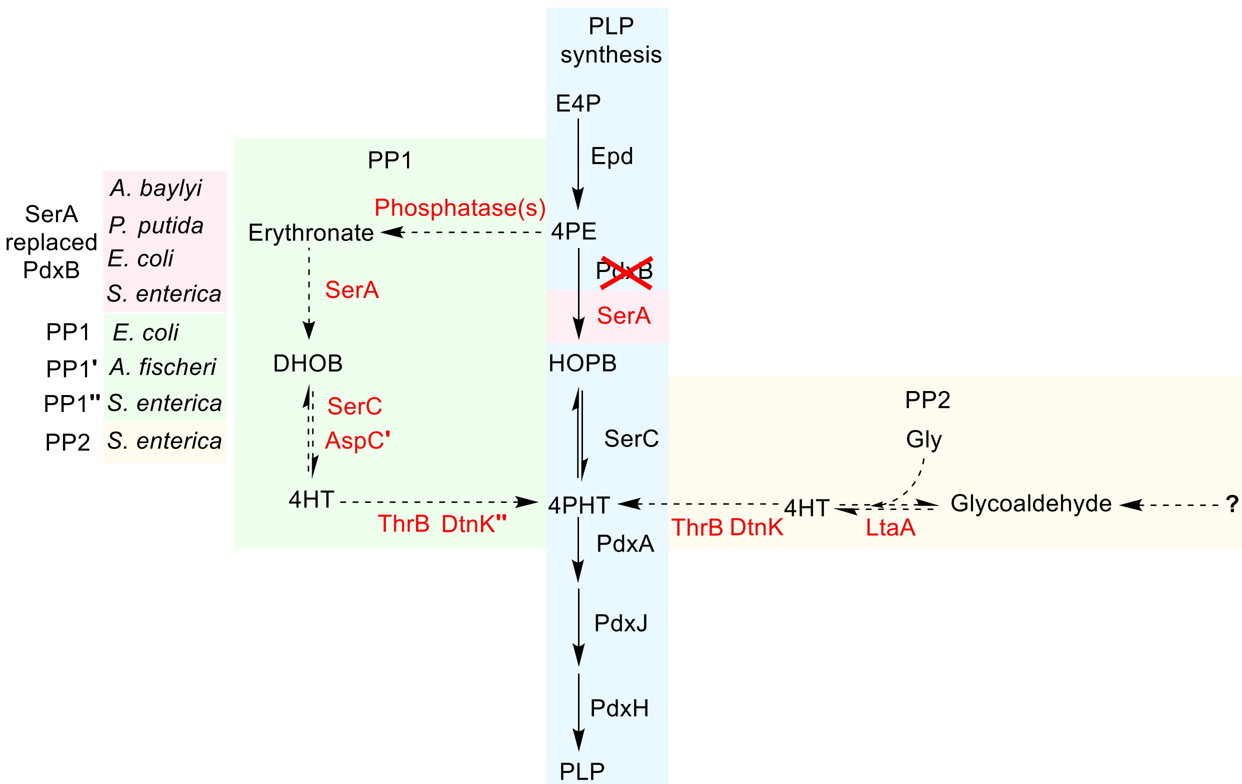

Figure 17. Mechanisms for PLP synthesis in Δ*pdxB* bacteria. Enzymes in black perform their native reaction; enzymes in red perform promiscuous reactions. At minimum one isolated strain restored PLP synthesis by replacing PdxB with SerA in *A. baylyi, P. putida, E. coli*, and *S. enterica*. At least one isolated strain in *E. coli, A. fischeri*, and *S. enterica* restored PLP synthesis with a version of PP1. AspC labeled with ' is only involved in PP1'; DtnK labelled with " is only involved in PP1". Enzymes in red without an apostrophe are involved in all versions of PP1. *S. enterica* additionally evolved the PP2 pathway.

Unlike *A. baylyi*, the growth rate of Δ*pdxB P. putida* improved during laboratory evolution, but the parental Δ*pdxB* strain exhibited slow growth on minimal medium. *P. putida* SerA has a high k_{cat}/K_M with 4PE, about 100-fold higher than its k_{cat}/K_M with erythronate. The high activity of SerA with 4PE and the requirement for SerA but not SerC or ThrB (which are required for PP1) for PLP synthesis in evolved Δ*pdxB P. putida* strains shown by Daniel Yoshimura suggest that SerA replaced the function of PdxB (**Figure 17**). Every evolved strain acquired a mutation in *glyAII*, which encodes serine hydroxymethyltransferase (GlyA11). Additional investigation is required to determine how mutations in *glyA11* affect PLP synthesis.

A. fischeri SerA enzymes had no activity with 4PE, and I determined SerA did not replace the function of PdxB. The strong selection for mutations in *serA* that increase the promiscuous activity of SerA on erythronate support the conclusion from genetic studies that PLP synthesis is restored by increasing flux through the PP1' pathway (**Figure 17**). Additionally, flux through PP1' synthesis in *A. fischeri* was likely increased by loss of function mutations in *yidA* and a mutation decreasing SerA inhibition by serine.

Δ*pdxB E. coli* and Δ*pdxB S. enterica* both required a longer evolution in minimal medium than *A. baylyi*, which required none, and *P. putida*. Δ*pdxB E. coli* and Δ*pdxB S. enterica* represent interesting cases where multiple strategies were used to restore PLP synthesis. The wild-type enzymes in both organisms have modest activity with 4PE, with *S. enterica* SerA having 10-fold greater activity than *E. coli* SerA. In evolved strain *Se3* and possibly in some so-far uncharacterized evolved strains of Δ*pdxB E. coli,* it appears SerA did replace PdxB. However, other strategies to restore PLP synthesis also appeared in these bacteria, both of which evolved versions of PP1. *S. enterica* additionally evolved another not yet fully characterized pathway PP2 (**Figure 17**).

The evolutionary trajectories in Δ*pdxB E. coli* and Δ*pdxB S. enterica* introduce the question of why these bacteria evolved multiple protopathways. The promiscuous activity of SerA on 4PE was in between the levels of high activity seen in *A. baylyi*/ *P. putida* and the undetectable activity in *A. fischeri*. The replacement of PdxB with SerA might be seen as the better option because it only involves one enzyme. However, Δ*pdxB E. coli* and Δ*pdxB S. enterica* both evolved versions of PP1 and did the irreversible phosphatase step converting 4PE to erythronate impact this? The presence of the irreversible step in PP1 converting 4PE to erythronate did not appear important in *A. baylyi* and *P. putida*. However, if the rate of 4PE dehydrogenation by SerA is very low, more 4PE may be shunted toward erythronate, setting the stage for further conversion of erythronate to 4PHT via PP1.

Chapter V

Conclusion

The understanding of how novel metabolic pathways evolve has increased with the formulation of the patchwork model. The majority of direct evidence supporting the patchwork model has come from bioinformatic data but leaves questions regarding how the process is carried out unanswered. Recent advances in synthetic biology have since reinforced the idea that enzymes can be patched together to form metabolic pathways through the creation of synthetic pathways that utilize the native and promiscuous activities of enzymes (Chen et al. 2019). While these achievements support the patchwork model, they do not provide insight into what dictates the evolutionary trajectory of a novel metabolic pathway, why some pathways form instead of others, and if this is contingent on pre-existing enzymes.

The laboratory evolution of a metabolic pathway allows for the characterization of the entire process and determination of why one metabolic pathway evolved instead of another. The model system of bacterial organisms lacking PdxB in the canonical PLP biosynthesis pathway allows the Copley lab to study the evolution of a metabolic pathway and how this process differs across organisms. In this work I characterized the evolution of a metabolic pathway in *Aliivibrio fischeri* and studied the catalytic activities of an enzyme essential to PLP restoration in many Δ*pdxB* evolved strains. The characterized pathway in *Aliivibrio fischeri* provides comparisons between the evolutionary solutions achieved by different Δ*pdxB* bacteria and shows that the PP1' pathway is similar to a pathway that evolved in Δ*pdxB E. coli* and *S. enterica*. The SerA enzyme assays confirmed the wild-type *A. baylyi* and *P. putida* SerA enzymes have a high promiscuous activity on 4PE and are consistent with the replacement of PdxB by SerA in these strains. The assays also reinforced that *A. fischeri, E. coli,* and *S. enterica* evolved alternative strategies for PLP restoration because their SerA enzymes have low or no activity with 4PE. The SerA enzyme assays revealed the promiscuous activities of SerA influenced the evolution of PLP restoration in Δ*pdxB* bacteria restored PLP synthesis.

Primary questions

Is there a contingency on pre-existing enzymes?

Pre-existing enzymes being required for the evolution of a novel metabolic pathway may seem intuitive, however, that has been a lingering question. In the case of PLP restoration in Δ*pdxB* *A. fischeri*, SerA did not replace PdxB and mutations in SerA allowing for this did not arise. This is likely because SerA had no activity with 4PE from the start, and instead the mutations that were selected for in *serA* improved the already present promiscuous activity on erythronate. The solution for PLP synthesis restoration in *A. fischeri* was contingent on the availability of a pre-existing promiscuous activity. Other bacteria also took advantage of the availability of promiscuous activities. However, promiscuous activities are not the only factor that influences the evolution of a metabolic pathway. The multiple solutions that arose in *E. coli* and *S. enterica* show the repertoire of enzymes and catalytic and promiscuous activity of those enzymes does not entirely dictate the evolutionary trajectory of a metabolic pathway.

How do rate-limiting enzymes influence the evolution of metabolic pathways?

The evolution of a novel metabolic pathway can be limited to the promiscuous activity of an enzyme, referred to as the rate-limiting enzyme. The rate-limiting enzyme decreases metabolic flux through the pathway and prevents flux from increasing to physiologically relevant levels. Many factors can influence the flux through a metabolic pathway and identifying the mutations that arise during evolution and the catalytic activities of enzymes in the pathway can help reveal what the rate-limiting enzyme is and if this differs across organisms. In *A. fischeri*, mutations in *serA* improved the activity of SerA on erythronate and indicate that the promiscuous activity of SerA limited the restoration of PLP synthesis. Additionally, the mutations in *yidA* likely increased flux into PLP synthesis. These mutations could have allowed *A. fischeri* to further overcome the low promiscuous activity of SerA with erythronate. The mutations that arose in *serA* and *gapA* in *E. coli* indicate SerA was the rate-limiting enzyme to PLP synthesis in Δ*pdxB E. coli* but restores PLP synthesis in multiple ways. *S. enterica* SerA has a higher activity with 4PE than *A. fischeri*, but lower than *A. baylyi* and *P. putida* and does not always restore PLP synthesis by replacing PdxB with SerA. *E. coli and S. enterica* show that while the level of activity with 4PE influenced the accessibility to different methods of PLP synthesis, there were different factors, likely specific mutations that arose during evolution, that influenced the evolutionary trajectories of each Δ*pdxB* strain.

The impact of metabolic pathway evolution

The laboratory study of metabolic pathway evolution provides concrete evidence to support the patchwork model and helps explain why different organisms evolve different solutions to the same environmental challenge. Additionally, research in this field has shown how the same species with the same repertoire of enzymes can evolve different solutions to the same challenge. The rise in microbes with the ability to degrade plastics and harmful chemicals released into the environment by humans shows the ability of life to generate novel metabolic pathways to adapt to a changing environment.

Chapter V

Methods

General methods

Biological resources

Strains, plasmids, and primers used in this work are listed in the Appendix in **Tables A-1**, **A-2**, and **A-3**, respectively.

Reagents

Chemical reagents (antibiotics, IPTG, amino acids, tryptone, etc.) and media (LB and SOC) were purchased from Sigma-Aldrich and Thermo-Fischer. Enzymes used for PCR and plasmid construction were purchased from NEB. Primers were obtained from IDT, Eurofins genomics, and Thermo-Fischer. The 2X Gibson master mix was purchased from NEB and the homemade Gibson master mix used was made according to **Table 8.**

Table 8. Homemade Gibson master mix recipe. Recipe yields 25 x 15 µL aliquots.

Reagent	Amount
5x isothermal rxn buffer	100 µL
40 U/µL Taq DNA Ligase	50 µL
1 U/µL T5 Exonuclease	2 µL
2 U/µL Q5 Hi-Fi DNA Polymerase	6.25 µL
H2O	216.75 µL

Gibson assembly

All created plasmids in this work were made by Gibson Assembly (Gibson et al. 2009) and transformed into *E. coli* DH5α using the *E. coli* transformation method described below. Primers listed in Table A-3 were used to amplify template DNA (plasmid 1-10 ng, genomic 50-250 ng) using NEB Q5 High-Fidelity DNA Polymerase (M0492L), unless noted otherwise with Phusion High-Fidelity DNA Polymerase (M0530S). Standard 50 µl reactions were performed using manufacturer's instructions with the thermocycler settings listed in **Tables 9** and 10. Annealing temperatures were determined using the NEB Tm online calculator.

Table 9. PCR conditions used for Q5 polymerase.

Step	Temperature	Time
Initial denaturation	98°C	30 seconds
30 cycles, denature, anneal, amplify	98°C	10 seconds
	50-72°C	30 seconds
	72°C	30 seconds/kb
Final extension	72°C	2 minutes
End	4°C	

Table 10. PCR conditions used for Phusion polymerase.

Step	Temperature	Time
Initial denaturation	98°C	30 seconds
30 cycles, denature, anneal, amplify	98°C	10 seconds
	50-72°C	30 seconds
	72°C	30 seconds/kb
Final extension	72°C	10 minutes
End	4°C	

A 5 µl aliquot of all amplicons created using PCR were visualized under UV using electrophoresis on a 1% agarose gel run for 20 minutes at 130V using a 5 µl aliquot following the PCR reaction to ensure the fragments lacked contaminated amplified DNA.

The amplicons were then cleaned using the NEB (T1030L) PCR cleanup kit. Amplicons of antibiotic resistance markers and plasmid backbones, which were amplified from a plasmid containing the same antibiotic resistance marker, were additionally subjected to digestion by Dpn1 (NEB R0176S) to remove residual template plasmid. These amplicons were eluted in 44 µl of diH2O following PCR cleanup. 5 µl of 10X CutSmart buffer and 1 µl of DpnI were added to the eluted fragments and the reaction was incubated at 72°C for 3 h. Following digestion, the fragments were cleaned again with the NEB PCR cleanup kit and quantified using Qubit (Thermo Q32850).

The Gibson reactions were assembled with the fragments mixed to a maximum pmol of 0.5 in equimolar ratios for similar sized fragments or 1:3 molar ratios with the smaller fragment in excess. The fragment mixture volume was increased to 5 µl with diH2O once the maximum pmol was reached and added to either 5 µl 2X Gibson Assembly master mix (NEB E2611L) or 15 µl homemade Gibson Assembly master mix. The reactions were incubated at 50°C for 12 h followed by dialysis against 17.4 MΩ ultrapure H2O on an MCE membrane filter (0.025 µm pore size, VSWP02500) to remove salts prior to transformation.

E. coli DH5α cells were prepared and transformed with the dialyzed Gibson Assembly reaction using electroporation using a previously described procedure (Widney et al., 2024; Yang et al., 2024). The cells were then recovered with SOC at 37 °C for 1.5 h and plated on LB agar with appropriate antibiotics and incubated at 37°C overnight. The following day colonies were screed for transformants by colony PCR.

Splicing by overhang extension (SOE) PCR

The linear DNA fragment used to delete *thrB* in *A. fischeri* was constructed using a SOE PCR of three DNA fragments one *cmR* cassette flanked with two 1.5 kb homology arms for the upstream and downstream gene. The first step for the SOE amplified the homology arms using primers listed in **Table A-3** from *A. fischeri* gDNA and the *cmR* cassette from pKAW002 listed in **Table A-2**. The primers flanking the interior (connecting) ends of the 3 fragments had a 20 bp overhang, homologous to the fragment it will connect to. The 3 PCR amplified fragments are then mixed and subsequent PCR cycles will anneal the fragments together. The fragment is now fully made. Primers that only bind to the ends of the fully assembled fragment are then used in a subsequent PCR reaction for amplification of the product.

Colony PCR

Transformed colonies which arose on rich medium with appropriate antibiotics, following plasmid electroporation or genome editing, were screened using colony PCR. Colonies were picked and resuspended in 10 µl phosphate buffered saline (PBS). The OneTaq polymerase (NEB M0486L) master mix was mixed with appropriate primers listed in **Table A-3** according to manufacturer's instructions and the mixed reaction was aliquoted out into 6 µl reactions. 0.5 µl of the suspended colonies were added to the reactions and run in the thermocycler according to the amplification settings listed below in **Table 11**. Annealing temperatures were determined using the NEB Tm online calculator. A 3 µl aliquot of each reaction was run using electrophoresis on a 1% agarose gel and visualized under UV.

Table 11. PCR conditions used for colony PCR with OneTaq polymerase.

Step	Temperature	Time
Initial denaturation	94°C	5 minutes
30 cycles, denature, anneal, amplify	94°C	30 seconds
	45-68°C	30 seconds
	68°C	1 minute/kb
Final extension	68°C	5 minutes
End	4°C	

Positively screened amplicons were treated with ThermoFisher ExoSap-IT Express (75001) with the leftover colony PCR reactions and verified through Sanger sequencing using sequencing or external primers listed in **Table A-3.** Positively screened amplicons following Gibson Assembly were additionally screened using whole plasmid sequencing following the growth of the resuspended colony in PBS in liquid LB containing appropriate antibiotics. Successfully grown colonies in LB were prepped using the Monarch Plasmid Miniprep Kit (NEBT1010).

Bacterial growth

All bacterial strains were grown according to **Table 12** unless noted otherwise. All amino acid supplementation used concentrations listed in **Table 13**. Recipes for one-liter LBS/tris, SWTO, TMM, and MMM are listed in **Table 14**. All liquid minimal media used in this work, including TMM and MMM, were made fresh each day of use to avoid decreases in cell viability caused by old media, which begins after 24-30 h of stored liquid TMM and MMM. TMM plates were also

made fresh for each day of use for optimal growth.

Table 12. Growth conditions for *E. coli* and *A. fischeri*. Ampicillin (amp); chloramphenicol (chl); kanamycin (kan); gentamycin (gm); erythromycin (eyr).

Bacterial Species	**Undefined rich medium**	**Minimal medium**	**Temp. (°C)**	**Antibiotic concentrations (μg/mL)**					
					amp	chl	kan	gm	eyr
				Solvent	H_2O	100% EtOH	H_2O	H_2O	DMSO
E. coli	Lysogeny broth (LB)	M9	37		100	20	50	20	
A. fischeri	Lysogeny broth salt (LBS/tris), Saltwater tryptone (SWTO)	Tris minimal medium (TMM), Mops minimal medium (MMM)	28	SWTO		1	300	200	60
				TMM		1	200	100	60
				MMM		1	300	100	60

Table 13. **Amino acid supplementation concentrations for *E. coli* in M9 and *A. fischeri* in TMM and MMM.**

	A. fischeri	***E. coli***		***A. fischeri***	***E. coli***
	Optimal Concentration (mM)	**Optimal Concentration (mM)**		**Optimal Concentration (mM)**	**Optimal Concentration (mM)**
glycine	10	0.8	L-leucine	4	0.8
L-alanine	0.8	0.8	L-lysine	0.04	0.4
L-arginine	26	5.2	L-methionine	1	0.2
L-asparagine	2	0.4	L-phenylalanine	0.04	0.4
L-aspartate	4	0.4	L-proline	0.04	0.4
L-cysteine	0.2	0.1	L-serine	1	10
L-glutamate	0.06	0.6	L-threonine	0.4	0.4
L-glutamine	6	0.6	L-tryptophan	0.1	0.1
L-histidine	0.02	0.2	L-tyrosine	0.02	0.2
L-isoleucine	2	0.4	L-valine	0.06	0.6

Table 14. **Media recipes for growth of *A. fischeri* cultures.** Recipes are for 1L liquid media.

LBS/tris		**SWTO**		**TMM**		**MMM**	
Reagent	Amount	Reagent	Amount	Reagent	Amount	Reagent	Amount
LB	20 g	tryptone	5 g	tris pH 7.5	100 mL	MOPS pH 7.5	100 mL
NaCl	10 g	yeast extract	3 g	5M NaCl	60 mL	5M NaCl	60 mL
diH_2O	up to 1L	NaCl	10 g	1 M $MGSO_4 * 7H_2O$	50mL	1 M $MGSO_4 * 7H_2O$	50 mL
tris pH 7.5	10 mL	instant ocean*	25 g	33 mM K_2HPO_4	1 mL	333 mM K_2HPO_4	1 mL
		diH_2O	up to 1 L	10 mM $FeNH_4SO_4$	1 mL	10 mM $FeNH_4SO_4$	1 mL
				20% NH_4Cl	5 mL	20% NH_4Cl	5 mL
				20% D-glucose	20 mL	20% D-glucose	20 mL
				1M KCl	10 mL	1M KCl	10 mL
				1M $CaCl_2 * 2H_2O$	10 mL	1M $CaCl_2 * 2H_2O$	10 mL
				diH_2O	743 mL	diH_2O	743 mL

A. fischeri general methods

Minimal medium

The maximum OD_{600} reached by *A. fischeri* in TMM is only 0.2-0.4. To improve growth yield, Daniel Yoshimura combined two minimal media TMM, and a defined artificial seawater (DAS) minimal medium for *A. fischeri*, from the Ruby lab when located at the University of Hawai'i-Mānoa. Additionally, he changed the Tris buffer to MOPS buffer, with a buffering range of pH 6.5 to 7.9, optimal for *A. fischeri* growth. The new medium is referred to as MMM (MOPS minimal medium).

Growth environment

A. fischeri is sensitive to O_2 levels in the medium. *A. fischeri* cultures in 150 mL baffled flasks reach the highest OD_{600} of 2.4 in SWTO, 1.6 in LBS/tris, and 0.4 in TMM compared to growth in 48-well plates. Cultures in 48-well plates reach OD_{600} of 1.3 in SWTO, 0.9 in LBS/tris, and 0.1 in TMM. Increased growth correlates with increased levels of oxygenation. All work was carried out in 150 mL baffled flasks whenever possible to provide the highest level of aeration for the cultures.

Antibiotic concentrations

Growth assays were conducted to determine appropriate antibiotic concentrations in different types of media. Growth assays were conducted as follows. Five µl of *A. fischeri* ES114 was inoculated from a frozen glycerol stock into SWTO and incubated at 28 °C for 14 h with shaking. An aliquot of the culture was added to the appropriate medium to an OD_{600} of 0.001 and aliquoted into 15 mL culture tubes. Varying antibiotic concentrations were added to the cultures, and the cultures were incubated at 28 °C for 24 h with shaking. OD_{600} measurements were taken the following day to determine the minimum inhibitory concentration of each antibiotic in each medium type. The minimum inhibitory concentrations were doubled for this work to ensure full growth is abolished.

Amino acid supplementation

The growth assays I performed in Chapter I required growth of *A. fischeri* strains with genomic deletions in minimal medium. I determined appropriate concentrations of amino acids to use in *A. fischeri* by performing toxicity tests using the amino acid concentrations for EZ defined rich medium in *E. coli* (Neidhardt et al. 1974) at 1x, 10x, 0.2x and 0.1x.

Wild-type *A. fischeri* ES114 was streaked from a frozen glycerol stock onto SWTO/agar plates and incubated at 28 °C for 48 h. Single colonies were inoculated into 20 mL TMM in 150 mL baffled flasks for optimal aeration and growth. Amino acids were added individually to separate cultures, and cultures were incubated at 28 °C for 24 h with shaking. Following incubation, OD_{600} measurements were taken to determine the effect of each concentration of amino acid. OD_{600} measurements showed maximum usable concentrations in *A. fischeri* without reducing growth.

I used the amino acid concentrations listed in **Table 13** to determine the appropriate combination of amino acids to supplement growth in TMM of *A. fischeri* strains with *thrB*, *serA*, *serC*, and *aspC* deletions. I supplemented the medium with L-threonine for strains lacking *thrB* and L-serine for strains lacking *serA*. The Δ*serC* strain required additional supplementation tests because supplementation would inhibit SerA, which might affect PLP synthesis. The Δ*serC* strains were supplemented with glycine, L-cysteine, and L-tryptophan in the medium. The *aspC* gene is essential in *A. fischeri;* a Δ*aspC* strain cannot grow in TMM. I conducted a series of tests combining every amino acid while lacking one amino acid to determine which are essential for growth in TMM. This confirmed that all the amino acids at the concentrations listed in **Table 13** can be used together to create a defined minimal medium for *A. fischeri*. These tests showed that the Δ*aspC* strain required supplementation with L-aspartate, L-phenylalanine, and L-tyrosine.

A. fischeri genetic manipulation

A. fischeri genetic manipulation was carried out using an optimized method of a linear fragment deletion protocol outlined by (Christensen et al. 2020).

Creating a tfoX overexpressing strain

The linear fragment deletion protocol utilizes the natural competency of *Aliivibrio* species for genetic manipulation. *Aliivibrio* species are naturally competent under certain environmental conditions of nutrient limitation, high cell density, and chitin rich mucus. Chitin is comprised of polymer chains of N-acetylglucosamine. N-acetylglucosamine molecules upregulate the gene *tfoX* that controls the uptake and recombination processes of external DNA with the *Aliivibrio* chromosome (Pollack-Berti et al. 2010; Visick et al. 2018; Cohen et al. 2021).

A. fischeri needs to be directly exposed to chitin or N-acetylglucosamine molecules in the media to induce genetic competency. Chitin and N-acetylglucosamine are both very expensive to purchase. Instead, the *tfoX* was artificially overexpressed using a plasmid (Cohen et al. 2021). The plasmid, pLostfoX-Kan, was purchased from the paper from which this protocol was created (Christensen et al. 2020). The kanamycin resistance cassette was exchanged for a gentamycin resistance cassette with a two-piece Gibson assembly as described previously. The backbone was amplified from pLostfoX-Kan (**Table A-2**) and the gentamicin resistance cassette was amplified from pJH110 (**Table A-2**). The Gibson assembled plasmid was transformed into DH5a cells and screened, as described in the methods below. The resulting plasmid was pLostfoX-Gm **(Table A-2)**. pLostfoX-Gm was sequence verified and used to proceed with the linear fragment deletion protocol for creating the *A. fischeri tfoX* overexpressing strains.

A. fischeri strains of interest in this work include the wild-type *A. fischeri* ES114, *A. fischeri pdxB*::*kanR serA** L19F (*Af1*), and *A. fischeri pdxB*::*kanR yidA** E83* (*Af2*). The pLostfoX-Gm plasmid was transformed into the strains using a previously described di-parental mating method (Elston et al. 2023). The plasmid was first transformed into mu free donor λ pir (MFDλpir, **Table A-1**) by electroporation and introduced to strains of *A. fischeri* by using conjugation with MFDλpir. MFDλpir requires the molecule Diaminopimelic acid (DAP) to grow which allows for selection against *E. coli* following conjugation (Elston et al. 2023). Growth conditions for this protocol were changed to LBS/DAP for the conjugation plating to facilitate growth of both species of bacteria, followed by growth on SWTO/kan to only select for *A. fischeri* colonies with pLostfoX-Gm.

Linear fragment deletion protocol

The majority of genomic deletions performed used growth in TMM. However, the standard minimal medium for the protocol was changed to MMM. MMM allows for growth to a higher final OD_{600} and should be used instead of TMM for this method because of higher transformation frequency levels.

The strains that maintain the pLostfoX-Gm plasmid are considered *tfoX* overexpressing and the natural competence is induced by the constitutive promoter used for *tfoX*. The *A. fischeri* strains with pLostfoX-Gm were streaked out the strains on SWTO/agar/gm. Single colonies were inoculated into 5 mL TMM or MMM/ 10 µM pyridoxine in culture tubes and incubated at 28 °C for 14 h with shaking. Pyridoxine was added to support growth in TMM or MMM for *Af1* and *Af2*. After the 14 h incubation, OD_{600} was measured. Cultures that had reached an OD_{600} between 0.05-0.10 (mid-log phase) were optimal to proceed. The cultures were then diluted to an OD_{600} of 0.01 in 20 mL TMM or MMM/10 µM pyridoxine and appropriate amino acid supplementation in 150 mL baffled flasks and incubated at 28 °C with shaking. The larger volume of 20 mL allows for frequent OD_{600} measurements, and the 150 mL baffled flasks allow better aeration to assist with cell growth. OD_{600} was monitored periodically to determine when the OD_{600} reached 0.035 - 0.05 (mid-log phase). Transformations carried out at values of $OD_{600} > 0.05$ proved unsuccessful.

Linear DNA fragments containing an antibiotic resistance cassette with 1.5 kb upstream and downstream homology arms flanking the gene targeted for deletion are used for transformation. The linear DNA fragments for deletion of *thrB* was created by splicing-by-overlap-extension (SOE) and the linear DNA fragments for deletion of *serA*, *serC*, and *aspC* by Gibson assembly. Primers are listed in Table A-3. Fragments were amplified using PCR with NEB Q5 High-Fidelity DNA Polymerase (M0492L) followed by the NEB PCR cleanup kit and eluted in Qiagen buffer. Fragment samples were concentrated using a Labconco Centrivap Concentrator to yield 10 µl of linear DNA fragment at > 100 ng/µl.

Once the cultures reach early log phase at an OD_{600} of 0.35 – 0.5, 500 µl of culture was transferred to an Eppendorf tube. Ten µl of linear DNA deletion fragment at > 100 ng/µl was added to the Eppendorf, vortexed for 3 s to ensure proper mixing, and incubated at room temperature for 30 min without agitation to allow cells to take up DNA. The cells were then transferred to a 15 mL tube containing 500 µl LBS/Tris and incubated at 28 °C for 3 h with shaking. LBS/Tris was used as the rich medium in this step to decrease the lag phase during recovery. A recovery time of 12 h is recommended when prior growth occurred in TMM. Increasing the recovery time can increase the number of transformants for difficult deletions.

Following recovery, 400 µl and 100 µl of the cultures were plated on SWTO agar plates with chloramphenicol (1 µg/mL) for deletions of *thrB*, *serA*, and *serC* and with erythromycin (60 µg/mL) for deletion of *aspC*. Antibiotics were used to select for colonies that had undergone homologous recombination of the linear DNA fragment. The plates were incubated at 28 °C for 4-6 days. Colonies appear after day 2 when plated on medium containing erythromycin (60 μg/mL) and after day 3 when plated on medium containing chloramphenicol (1 μg/mL). The colonies were re-streaked on new plates and the new colonies were screened for the gene deletion using colony PCR with primers listed in **Table A-3.** Saved Colony PCR product of promising transformant samples were cleaned using ExoSAP-IT PCR Product Cleanup Reagent (78201) from ThermoFischer Scientific and sent for Sanger sequencing to verify the deletion.

Growth assays

A. fischeri strains used in growth assays were streaked from frozen glycerol stocks onto SWTO/agar with chloramphenicol for strains with deletions in *thrB*, *serA*, *serC* and erythromycin for strains with deletions in *aspC* and incubated at 28 °C for 48 h. Three single colonies were picked and resuspended in flasks containing 20 mL TMM/glucose with 10 μM pyridoxine and appropriate amino acid supplementation for strains with gene deletions. Amino acid supplementation is described above with optimal concentrations for *A. fischeri* listed in **Table 13**. Cultures were incubated for 16-18 h at 28 °C with shaking. Once the cultures reached an OD_{600} of 0.01, the cells were harvested by centrifugation at 4500 g for 10 min. The cell pellet was resuspended in 1 mL TMM/glucose and centrifuged at 6000 g for 1 min. The supernatant was removed, and the process was repeated six more timed to remove residual pyridoxine from the medium. The cell pellets were resuspended in TMM/glucose to a normalized OD600 of 0.01. Five 10-fold serial dilutions were performed of the resuspended cells and 5 μl of each dilution was dropped onto TMM/glucose agar plates containing different conditions of with and without pyridoxine and/or amino acid supplementation. The drops dried and the plates were incubated at 28 °C for six days prior to imaging.

Synthesis and purification of 4PE

4PE was enzymatically synthesized and purified using an adapted procedure for the phosphorylation of sugars (Zhang et al., 2016). An initial solution of 40 mL was prepared to 4PE using D-erythronate kinase (DenK) to enzymatically phosphorylate D-erythronate. DenK was purified and quantified using the purification scheme and protein quantification method outlined below. The reaction solution contained 10 mM HEPES, pH 7.6, 2.5 mM $MgCl_2$, 62.5 mM KCl, 3.75 mM ATP, 62.3 mM PEP, and 75 mM D-erythronate. The amount of PEP used in the solution was decreased to be the limiting reagent to prevent contamination from PEP after purification. The solution pH was adjusted to 7.6 using 10M NaOH and 5 µM DenK kinase and 10 U/mL pyruvate kinase from rabbit muscle (Sigma) was added. The reaction was incubated with stirring at 25°C for 20 h.

Following incubation, the reaction was verified to reach completion using a PK/LDH (Sigma) assay. The solution was acidified to a pH of 2.0 using 2M aqueous HCl and concentrated in a rotovap at 35°C to 20 mL. The concentrated solution was filtered through a 0.44 µm filter. The filtrate was mixed with 20 mL ethyl acetate in a separatory funnel and the aqueous bottom phase was collected. This was repeated 2 more times, and the aqueous phases were pooled. The pH of the resulting aqueous solution was adjusted to pH 7.0 using 1M aqueous KOH. 766.26 mg (3 mmol) $Ba(OAc)_2$ and 40mL of ethanol were added to the solution to isolate the 4PE Ba^{2+} salt as a white precipitate. The precipitate was collected from centrifugation at 4500 g for 10 min. The collected precipitate was washed successively with 25 mL of each 2:1 EtOH/H2O, 100% EtOH, and 100% ethyl acetate.

The 4PE Ba^{2+} precipitate was dissolved in 20 mL H_2O pH 2.0 and 426mg (3 mmol) Na_2SO_4 was added to remove the barium salt as $BaSO_4$. The precipitated solution was centrifuged at 4500 g for 10 min and the white $BaSO_4$ was removed. The pH of the aqueous clear solution was adjusted to pH 7.0 using 5 M aqueous KOH. The solution was then concentrated to 4mL using rotovap at 35 °C for 10 min. The concentrated solution was run through a Dowex 1×2 resin (100-200 mesh, chloride form, Sigma) column using a gradient of 0-1 N aqueous NH_4HCO_3 on an Amersham Biosciences UPC-900 FPLC. Fractions were analyzed using a Molybdate reagent solution to identify the phosphate containing fractions and pooled accordingly. The pooled fractions were lyophilized using a rotovap at 35°C for 1 h followed by overnight incubation at 30°C to further dry the product. The resulting 4PE was a tacky cloudy white product. A small sample was sent for 1 H, 13 C NMR, and 31P NMR spectroscopy characterization and verified the purified 4PE product.

The 4PE was stored at -80°C until further use in enzymatic assays and dissolved in H_2O through vigorous mixing. The redissolved 4PE was quantified using a Molybdate reagent assay with a standard curve made using $NaPO_4$.

Protein Purification

Protein expression

Protein expression plasmids and expression strains are listed in **Table A-2** and **Table A-1** respectively. Protein specific methods including plasmid and strain construction and type of protein purification are described below for each protein.

Expression of all proteins were carried out as follows unless noted otherwise. 5 µl of frozen protein expressing cultures were inoculated in 10 mL LB/kan_{50}, to maintain protein expression plasmids, and grown at 37 °C for 12 h with shaking. Cultures were inoculated into one liter of TB (Terrific broth)/kan_{50} (LB/kan_{50} for SerA expression) with 200 µl antifoam O. Once the cultures reached an OD_{600} of 0.4-0.5, 1 mM isopropyl β- d-1-thiogalactopyranoside (IPTG) was added to induce protein expression and incubated at 25 °C with shaking for 16 h. Cells were harvested at 8000 g for 10 min at 4 °C and the cell pellet was saved at -20 ºC until purification.

Protein purification and affinity column preparation

Following expression, all proteins were prepared for purification as follows. The cell pellet was resuspended in 35 mL purification buffer A stored at 4 ºC. Protease inhibitor tablets were added (Thermo Scientific™ A32955) and shaken to dissolve. Lysozyme (1 mg/mL) was added and incubated at 4 °C for 1 h with gentle tumbling. Cells were then kept on ice and lysed by sonication with 5 cycles of 10 s on and 20 s off. Lysed cells were centrifuged at 20000 x g at 4 °C for 20 min for cell debris removal. The supernatant was saved, and the protein of interest was purified using column chromatography according to methods described specific to each protein.

ThrB expression and purification

ThrB expression plasmid was constructed using fragments of the *A. fischeri thrB* gene were amplified from *A. fischeri* gDNA using NEB Q5 High-Fidelity DNA Polymerase (M0492L) and primers listed in **Table A-3**. The fragments were cloned into a pET28 backbone with a His_6-tag (six histidines) at the N-terminus and a kanamycin resistance marker by a two-piece Gibson assembly. The backbone was amplified from pKAW050 listed in **Table A-2** with primers listed in **Table A-3**. The plasmid was sequence-verified and electroporated into *E. coli* NiCO21 *thrB*::*cmR* (**Table A-1**). The *thrB* gene was deleted in the expression strain by lambda Red recombination using a previously described protocol (Baba et al., 2006) to remove possible contamination of *E. coli* ThrB for enzyme activity assays. The ThrB protein was expressed and prepared for purification using the general procedure described above except for using a specific ThrB lysis buffer which consisted of 100 mM HEPES, pH 7.6, 10 mM $MgCl_2$, and 250 mM KCl, instead of ThrB purification buffer A.

Following centrifugation, The ThrB protein was purified from the isolated supernatant using a hand-packed Ni-NTA resin column procedure as follows. 300 µl bed volume (Cube Biotech 74105) nickel affinity resin was added to the supernatant. The solution was incubated at 4 °C for 1 h with gentle tumbling to assist with protein His_6-tag binding of the nickel resin. The protein-resin solution was centrifuged at 700 x g for 3 min and the resin was resuspended in 5 mL ThrB purification buffer A, consisting of 100 mM HEPES, pH 7.6 and 30 mM NaCl. Resuspended resin was transferred to a benchtop column to form the hand-packed IMAC column. ThrB protein was then purified using a stepped gradient of ThrB purification buffer A and buffer B with purification buffer B additionally containing 500mM imidazole. Protein elution was verified by SDS-page and fractions were pooled accordingly shown in **Figure 18**. Imidazole was removed from pooled fractions using overnight dialysis (Thermo scientific Slide-A-Lyzer Dialysis Cassette G2) in ThrB purification buffer A.

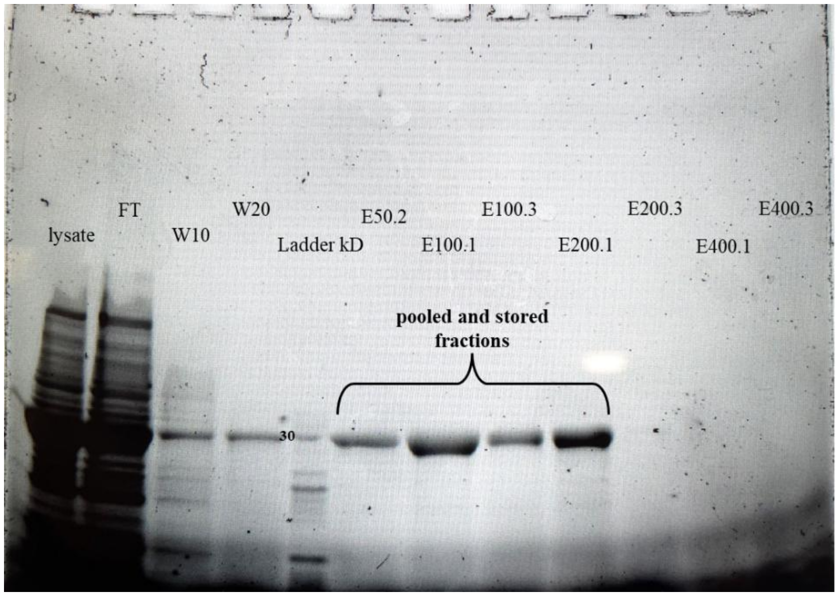

Figure 18. SDS-page gel of fraction collected during purification of his-tagged ThrB following IMAC. ThrB protein is about 30 kD.

DenK expression and purification

DenK expression plasmid was constructed using a gBlock from Twist Bioscience and cloned into a pET28 backbone with a His_6-tag (six histidines) at the N-terminus and a kanamycin resistance marker by a two-piece Gibson assembly. The backbone was amplified from pKAW050 listed in **Table A-2** with primers listed in **Table A-3**. The plasmid was sequence-verified and electroporated into *E. coli* NiCO21 (**Table A-1**). The DenK protein was expressed using the general procedure described above.

The DenK protein was expressed and prepared for purification using the general procedure described above and the DenK purification buffer A consisted of 20 mM HEPES, pH 7.5, 500 mM NaCl, and 10% glycerol. Following centrifugation, DenK was purified from the isolated supernatant using a pre-made Ni-NTA resin column (GE Healthcare HisTrap^{TM} FF) with a one mL bed volume to obtain a higher protein yield. The supernatant with DenK was loaded onto the column and purified using Amersham Biosciences UPC-900 FPLC using a linear gradient of DenK purification buffer A and buffer B, which is identical to buffer A and additionally contains 500 mM imidazole. Protein elution was verified by SDS-page and fractions were pooled accordingly shown in **Figure 19**. Imidazole was removed from pooled fractions using overnight dialysis (Thermo scientific Slide-A-Lyzer Dialysis Cassette G2) in DenK purification buffer A.

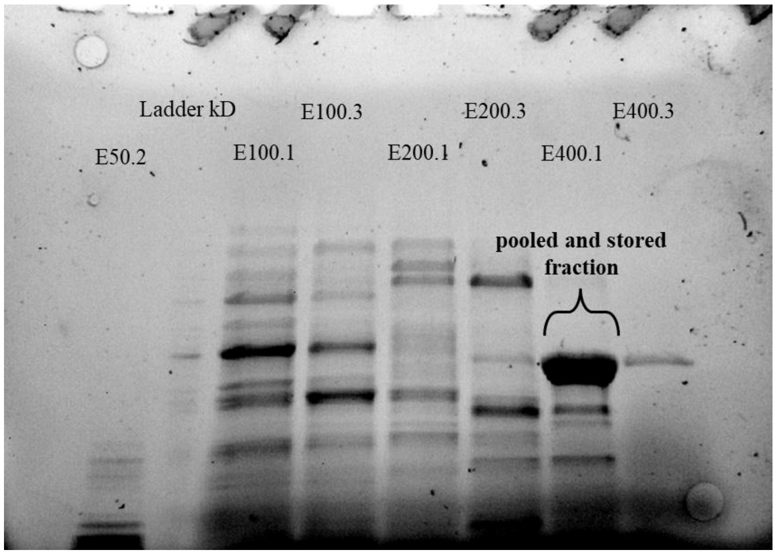

Figure 19. SDS-page gel of fraction collected during purification of his-tagged DenK following purification on the Ni-NTA resin column using FPLC. The ladder appears to have been degraded.

D2HGDH expression and purification

D-2-hydroxyglutarate dehydrogenase (D2HGDH) expression plasmid was constructed by (Juhan et al. 2019) and is comprised of a pET28 backbone with a His_6-tag (six histidines) at the N-terminus, a kanamycin resistance marker, and the D2HGDH gene from Pseudomonas stutzeri A1501. The plasmid was previously electroporated into *E. coli* BL21 *pdxB*::*cmR serA*::*cmR* (**Table A-1**) by Kim et al. 2019. The *pdxB* and *serA* genes were deleted in the expression strain by lambda Red recombination using a previously described protocol (Baba et al., 2006) to remove possible contamination of *E. coli* PdxB and SerA for SerA enzyme activity assays. The D2HGDH protein was expressed using the general procedure described above.

The D2HGDH protein was expressed and prepared for purification using the general procedure described above, and the 2HGDH purification buffer A consisted of 15 mM $NaHPO_4$, 4.9 mM NaH_2PO_4, pH 7.4, and 600 mM NaCl. Following centrifugation, D2HGDH was purified from the isolated supernatant using a pre-made Ni-NTA resin column (GE Healthcare HisTrap^{TM} FF) with a five mL bed volume to obtain a very high protein yield for its use as a coupling enzyme in the SerA assays. The supernatant with D2HGDH was loaded onto the column and purified using Amersham Biosciences UPC-900 FPLC using a linear gradient of D2HGDH purification buffer A and buffer B, which is identical to buffer A and additionally contains 500 mM imidazole. Protein elution was verified by SDS-page and fractions were pooled accordingly shown in **Figure 20**. Pooled fractions were concentrated down to two mL and imidazole was removed using 35000 MW spin columns (Merck Millipore Ltd. Amicon® Ultra-4 Centrifugal Filter Units).

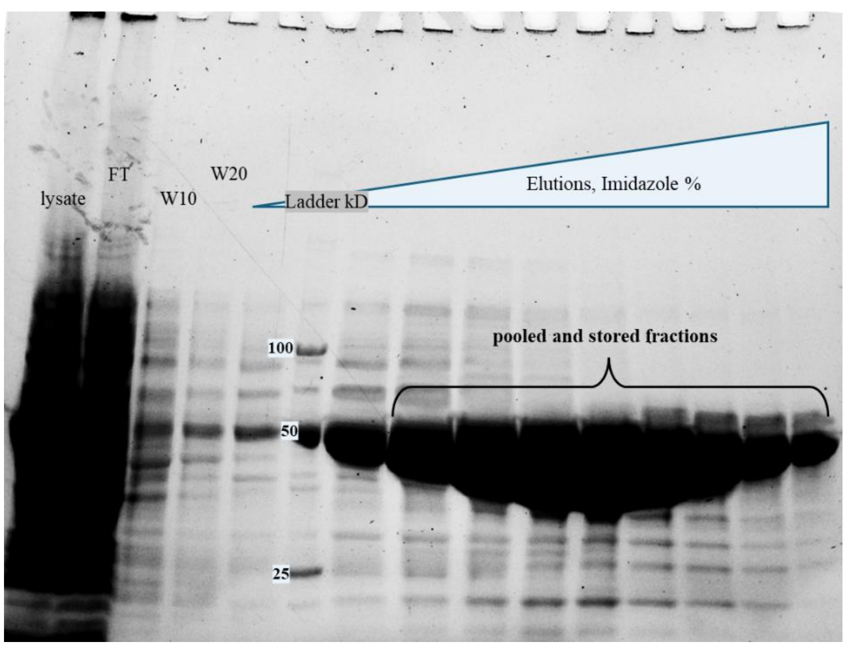

Figure 20. SDS-page gel of fraction collected during purification of his-tagged D2HGDH following purification on a Ni-NTA resin column using FPLC. D2HGDH protein is about 51 kD. D2HGDH lacks tryptophan residues and the SDS-page gel was stained with Coomassie blue dye prior to visualization.

ETFAB expression and purification

ETF A and ETF B (ETFAB) expression plasmid was constructed by Kim et al. 2019 and is comprised of a pET28 backbone with a His_6-tag (six histidines) at the N-terminus, a kanamycin resistance marker, and the ETF A and ETF B gene from Pseudomonas stutzeri A150. The plasmid was previously electroporated into *E. coli* BL21 *pdxB*::*cmR serA*::*cmR* (**Table A-1**) by Dr. Juhan Kim. The *pdxB* and *serA* genes were deleted in the expression strain by lambda Red recombination using a previously described protocol (Baba et al., 2006) to remove possible contamination of *E. coli* PdxB and SerA for SerA enzyme activity assays. The ETFAB proteins were expressed using the general procedure described above.

The ETFAB protein was expressed and prepared for purification using the general procedure described above, and the ETFAB purification buffer A consisted of 15 mM $NaHPO_4$, 4.9 mM NaH_2PO_4, pH 7.4, and 600 mM NaCl. Following centrifugation, ETFAB was purified from the isolated supernatant using a pre-made Ni-NTA resin column (GE Healthcare HisTrap™ FF) with a five mL bed volume to obtain a very high protein yield for its use as a coupling enzyme in the SerA assays. The supernatant with ETFAB was loaded onto the column and purified using Amersham Biosciences UPC-900 FPLC using a linear gradient of ETFAB purification buffer A and buffer B, which is identical to buffer A and additionally contains 500 mM imidazole. Protein elution was verified by SDS-PAGE and fractions were pooled accordingly shown in **Figure 21**. Pooled fractions were concentrated down to two mL and imidazole was removed using 10000 MW spin columns (Merck Millipore Ltd. Amicon® Ultra-4 Centrifugal Filter Units).

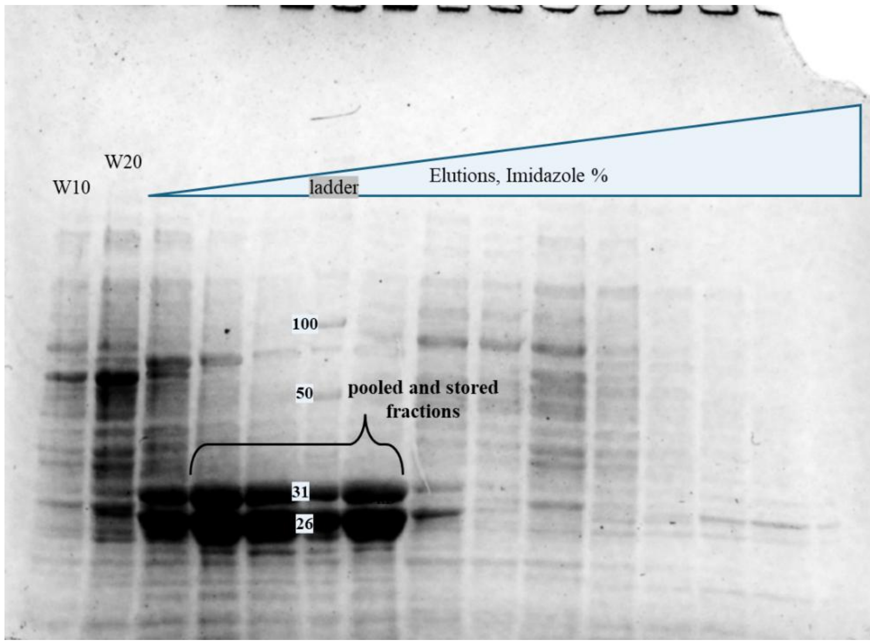

Figure 21. SDS-page gel of fraction collected during purification of his-tagged ETFAB following purification on a Ni-NTA resin column using FPLC. ETFA protein is about 31 kD and the ETFB protein is about 26 kD. ETFAB lacks tryptophan residues and the SDS-page gel was stained with Coomassie blue dye prior to visualization.

SerA expression and purification

SerA expression plasmids were constructed using fragments of *serA* genes amplified from appropriate gDNA listed in **Table A-2** using NEB Q5 High-Fidelity DNA Polymerase (M0492L) and primers listed in **Table A-3**. The fragments were cloned into a pET28 backbone with a His_6-tag (six histidines) at the N-terminus and a kanamycin resistance marker by a two-piece Gibson assembly. The backbone was amplified from pKAW050 listed in **Table A-2** with primers listed in **Table A-3**. The plasmid was sequence-verified and electroporated into *E. coli* BL21 *pdxB*::*cmR serA*::*cmR* (**Table A-1**). The *pdxB* and *serA* genes was deleted in the expression strain by lambda Red recombination using a previously described protocol (Baba et al., 2006) to remove possible contamination of *E. coli* PdxB and SerA for enzyme activity assays.

The SerA proteins were expressed using the general method above using LB instead of TB which was found to improve the stability of mutant SerA proteins from SDS-page gels run following purification. SerA proteins were purified using the same hand-packed Ni-NTA column procedure described above. SerA purification buffer A, and purification buffer B are comprised of 15 mM $NaHPO_4$, 4.9 mM NaH_2PO_4, pH 7.4, and 600 mM NaCl with buffer B additionally containing 500 mM imidazole. Following purification, protein elution was verified by SDS-page and fractions were pooled accordingly shown in **Figures A1-A20**. Pooled fractions for each protein were concentrated down to one mL and imidazole was removed using 35000 MW spin columns (Merck Millipore Ltd. Amicon® Ultra-4 Centrifugal Filter Units).

ThrB kinetic Assay

A. fischeri ThrB activity was measured using a coupled pyruvate kinase (PK) - lactate dehydrogenase (LDH) assay (**Figure 22**). 200 µl reactions were performed in clear 96-well plates. Reaction mixtures are displayed in **Table 15** and contained 10 mM HEPES-$MgCl_2$ 1 mM ATP, 1 mM phosphoenolpyruvate (PEP), 0.24 µM PK, 0.24 µM LDH, 0.25 µM NADH, 0.0025 µM ThrB for homoserine assays or 0.025 µM ThrB for 4HT assays, and varying amounts of homoserine or 4HT. Reactions were preincubated at 28 °C for five min, corresponding to the temperature at which *A. fischeri* was evolved, in a Varioscan plate reader and initiated with 40 µl of substrate, either homoserine or 4HT. Oxidation of NADH in the coupled assay was tracked through the change in absorbance at 340 nm and converted to molarity using $\varepsilon 340 = 6220\ M^{-1}cm^{-1}$. Initial velocities were recorded for the first 5% of the reaction and fitted to a Michaelis-Menten curve in GraphPad Prism 8.

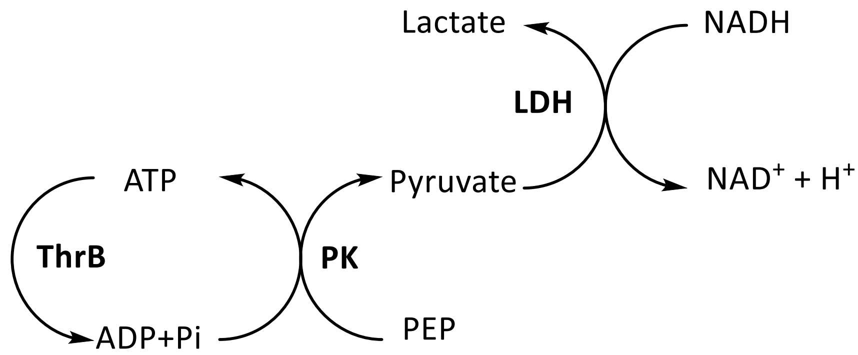

Figure 22. ThrB kinetic assay scheme using a PK-LDH coupled assay.

Table 15. ThrB kinetic assay reaction mixtures.

Compound	Stock concentration	Working concentration	Volume of stocks used for 200 µl reaction
HEPES-$MgCl_2$ pH 7.6	100 mM	10 mM	10 µl
Pyruvate kinase (PK)	6 mM	0.24 µM	8 µl
Lactate dehydrogenase (LDH)	12 mM	0.24 µM	4 µl
NADH	100 mM	1 mM	2 µl
ATP	100 mM	1 mM	2 µl
PEP	100 mM	1 mM	2 µl
ThrB	25 µM	0.0025 µM—Homoserine 0.025 µM—4HT	2 µl
diH2O			120 µl
Homoserine	0-40 mM	0-20 mM	40 µl
4HT	0-80 mM	0-40 mM	40 µl

SerA kinetic assay

SerA activity was measured using an adapted protocol from (Kim et al. 2019). SerA activity was measured using a four times coupled assay using α-ketoglutarate, D2-HGDH, ETFAB, and 2,6-dichlorophenolindophenol (DCIP) due to the recycling of NADH on the enzyme. 50 µl reactions were performed in clear 384-well plates. Reaction mixtures are displayed in **Table 16** and contained 200 mM HEPES-NaOH pH 7.4, about 20 µM D2HGDH, about 15 µM ETFAB, 1 mM NAD^+, 1 mM α-ketoglutarate, 0.15 mM DCIP, about 1 µM SerA, and varying concentrations of either 3-phosphoglycerate (3PG), erythronate, 4-phosphoerythronate (4PE), or 3PG with added serine for inhibition assays. DCIP stock concentration was made at 10 mM in diH2O at 35 °C to

fully dissolve the DCIP before addition to the reaction mixture. Reaction mixtures were first created as a larger master mix of 100-200 mL lacking all enzymes and substates to increase the pH from 6.9, which dropped due to the addition of NAD^+, back up to pH 7.4 using 10M NaOH. Once the master mix pH reached 7.4 again, coupling enzymes D2HGDH and ETFAB were added. The same master mix which lacked SerA and substrate was used for all reactions that day. SerA enzymes were thawed at room temperature and immediately added to small aliquots of the master mix prior to plate assay set up to prevent precipitation caused by storage at room temperature for over 30 min.

Table 16. SerA kinetic assay reaction mixtures.

Compound	Stock Concentration	Working Concentration	Volume of Stocks Used for 50 µL Reaction
HEPES-NaOH pH 7.4	2 M	200 mM	5 µl
D2HGDH	133 µM	20 µM	7.5 µl
ETFAB	100 µM	15 µM	7.5 µl
NAD^+	100 mM	1 mM	0.5 µl
α-ketoglutarate	100 mM	1 mM	0.5 µl
DCIP	10 mM	0.15 mM	0.75 µl
SerA	50 µM	1 µM	1 µl
diH_2O			17.25 µl
Substrate			
3PG	100 mM	0.25-20 mM	10 µl
Erythronate	800 mM	0.5-160 mM	10 µl
4PE	50 mM	10 mM	10 µl
L-serine + 3PG	200mM 200mM	0.078-2mM, 20mM 0.25-20 mM	5 µl 5 µl

SerA enzymes were assayed at the corresponding temperature to which the organism evolved, except for *A. fischeri* which was increased from 28 °C to 30 °C for ease of operations. Reactions were preincubated at (30 °C for *A. fischeri*, *A. baylei*, and *P. putida* SerAs and 37 °C for *S. enterica* and *E. coli* SerAs) for 3 min, in a Varioscan plate reader and initiated with 10 µl of substrate, either 3PG, erythronate, 4PE or 3PG with serine. Reduction of DCIP in the coupled assay was tracked through the change in absorbance at 600 nm and converted to molarity using ε600 = 22000 $M^{-1}cm^{-1}$. Initial velocities were recorded for the first 5% of the reaction and fitted to a Michaelis-Menten curve in GraphPad Prism 8 shown by representative **Figures 6** and **16**. Each day, all SerA enzymes and coupling enzymes were quantified using a Bradford assay to obtain accurate measurements across multiple days. The k_{cat}/k_M values calculated from the Michaelis-Menten curves were used to compare the activities of all SerA enzymes across multiple substrates displayed in **Table 6**.

References

Abramson J, Adler J, Dunger J, Evans R, Green T, Pritzel A, Ronneberger O, Willmore L, Ballard AJ, Bambrick J, et al. 2024. Accurate structure prediction of biomolecular interactions with AlphaFold 3. Nature. 630(8016):493–500. doi:10.1038/s41586-024-07487-w.

Berglund P, Humble MS, Branneby C. 2012. 7.18 C–X Bond Formation: Transaminases as Chiral Catalysts: Mechanism, Engineering, and Applications. In: Carreira EM, Yamamoto H, editors. Comprehensive Chirality. Amsterdam: Elsevier. p. 390–401. [accessed 2025 Mar 31]. https://www.sciencedirect.com/science/article/pii/B9780080951676007230.

Chen W, Yao J, Meng J, Han W, Tao Y, Chen Y, Guo Y, Shi G, He Y, Jin J-M, et al. 2019. Promiscuous enzymatic activity-aided multiple-pathway network design for metabolic flux rearrangement in hydroxytyrosol biosynthesis. Nat Commun. 10(1):960. doi:10.1038/s41467-019-08781-2.

Christensen DG, Tepavčević J, Visick KL. 2020. Genetic Manipulation of Vibrio fischeri. Curr Protoc Microbiol. 59(1):e115. doi:10.1002/cpmc.115.

Cohen JJ, Eichinger SJ, Witte DA, Cook CJ, Fidopiastis PM, Tepavčević J, Visick KL. 2021. Control of Competence in Vibrio fischeri. Appl Environ Microbiol. 87(6):e01962-20. doi:10.1128/AEM.01962-20.

Coton C, Talbot G, Le Louarn M, Dillmann C, de Vienne D. 2022. Evolution of enzyme levels in metabolic pathways: A theoretical approach. Part 1. J Theor Biol. 538:111015. doi:10.1016/j.jtbi.2022.111015.

Denise R, Babor J, Gerlt JA, de Crécy-Lagard V. 2023. Pyridoxal 5'-phosphate synthesis and salvage in Bacteria and Archaea: predicting pathway variant distributions and holes. Microb Genomics. 9(2):mgen000926. doi:10.1099/mgen.0.000926.

Ducat DC, Way JC, Silver PA. 2011. Engineering cyanobacteria to generate high-value products. Trends Biotechnol. 29(2):95–103. doi:10.1016/j.tibtech.2010.12.003.

Elston KM, Phillips LE, Leonard SP, Young E, Holley JC, Ahsanullah T, McReynolds B, Moran NA, Barrick JE. 2023. The Pathfinder plasmid toolkit for genetically engineering newly isolated bacteria enables the study of Drosophila-colonizing Orbaceae. bioRxiv.:2023.02.15.528778. doi:10.1101/2023.02.15.528778.

Fani R, Fondi M. 2009. Origin and evolution of metabolic pathways. Phys Life Rev. 6(1):23–52. doi:10.1016/j.plrev.2008.12.003.

Gupta RD. 2016. Recent advances in enzyme promiscuity. Sustain Chem Process. 4(1):2. doi:10.1186/s40508-016-0046-9.

Judge A, Dodd MS. 2020. Metabolism. Essays Biochem. 64(4):607–647. doi:10.1042/EBC20190041.

Kim J, Flood JJ, Kristofich MR, Gidfar C, Morgenthaler AB, Fuhrer T, Sauer U, Snyder D, Cooper VS, Ebmeier CC, et al. 2019. Hidden resources in the Escherichia coli genome restore PLP synthesis and robust growth after deletion of the essential gene pdxB. Proceedings of the National Academy of Sciences. 116(48):24164–24173. doi:10.1073/pnas.1915569116.

Kanehisa M. 2019. Toward understanding the origin and evolution of cellular organisms. Protein Sci. 28(11):1947–1951. doi:10.1002/pro.3715.

Kanehisa M, Furumichi M, Sato Y, Matsuura Y, Ishiguro-Watanabe M. 2025. KEGG: biological systems database as a model of the real world. Nucleic Acids Res. 53(D1):D672–D677. doi:10.1093/nar/gkae909.

Kanehisa M, Goto S. 2000. KEGG: Kyoto Encyclopedia of Genes and Genomes. Nucleic Acids Res. 28(1):27–30. doi:10.1093/nar/28.1.27.

Koper K, Han S-W, Pastor DC, Yoshikuni Y, Maeda HA. 2022. Evolutionary origin and functional diversification of aminotransferases. J Biol Chem. 298(8):102122. doi:10.1016/j.jbc.2022.102122.

Kuznetsova E, Proudfoot M, Gonzalez CF, Brown G, Omelchenko MV, Borozan I, Carmel L, Wolf YI, Mori H, Savchenko AV, et al. 2006. Genome-wide Analysis of Substrate Specificities of the Escherichia coli Haloacid Dehalogenase-like Phosphatase Family *. J Biol Chem. 281(47):36149–36161. doi:10.1074/jbc.M605449200.

Lazcano A, Díaz-Villagómez E, Mills T, Oró J. 1995. On the levels of enzymatic substrate specificity: Implications for the early evolution of metabolic pathways. Adv Space Res. 15(3):345–356. doi:10.1016/S0273-1177(99)80106-9.

Lazcano A, Miller SL. 1999. On the Origin of Metabolic Pathways. J Mol Evol. 49(4):424–431. doi:10.1007/PL00006565.

Morowitz HJ. 1999. A theory of biochemical organization, metabolic pathways, and evolution. Complexity. 4(6):39–53. doi:10.1002/(SICI)1099-0526(199907/08)4:6<39::AID-CPLX8>3.0.CO;2-2.

Neidhardt FC, Bloch PL, Smith DF. 1974. Culture Medium for Enterobacteria. J Bacteriol. 119(3):736–747.

Peña-Soler E, Fernandez FJ, López-Estepa M, Garces F, Richardson AJ, Quintana JF, Rudd KE, Coll M, Vega MC. 2014. Structural Analysis and Mutant Growth Properties Reveal Distinctive Enzymatic and Cellular Roles for the Three Major L-Alanine Transaminases of Escherichia coli. PLOS ONE. 9(7):e102139. doi:10.1371/journal.pone.0102139.

Pettersen EF, Goddard TD, Huang CC, Meng EC, Couch GS, Croll TI, Morris JH, Ferrin TE. 2021. UCSF ChimeraX: Structure visualization for researchers, educators, and developers. Protein Sci. 30(1):70–82. doi:10.1002/pro.3943.

Pollack-Berti A, Wollenberg MS, Ruby EG. 2010. Natural transformation of Vibrio fischeri requires tfoX and tfoY. Environ Microbiol. 12(8):2302–2311. doi:10.1111/j.1462-2920.2010.02250.x.

Rix G, Watkins-Dulaney EJ, Almhjell PJ, Boville CE, Arnold FH, Liu CC. 2020. Scalable continuous evolution for the generation of diverse enzyme variants encompassing promiscuous activities. Nat Commun. 11:5644. doi:10.1038/s41467-020-19539-6.

Schoenmakers LLJ, Reydon TAC, Kirschning A. 2024. Evolution at the Origins of Life? Life. 14(2):175. doi:10.3390/life14020175.

Schuller, D. J., Grant, G. A., & Banaszak, L. J. (1995). The allosteric ligand site in the Vmaxtype cooperative enzyme phosphoglycerate dehydrogenase. Nature Structural Biology, 2(1), 69–76.

Scossa F, Fernie AR. 2020. The evolution of metabolism: How to test evolutionary hypotheses at the genomic level. Comput Struct Biotechnol J. 18:482–500. doi:10.1016/j.csbj.2020.02.009.

Takemoto K. 2012. Current Understanding of the Formation and Adaptation of Metabolic Systems Based on Network Theory. Metabolites. 2(3):429–457. doi:10.3390/metabo2030429.

The UniProt Consortium. 2025. UniProt: the Universal Protein Knowledgebase in 2025. Nucleic Acids Res. 53(D1):D609–D617. doi:10.1093/nar/gkae1010.

Visick KL, Hodge-Hanson KM, Tischler AH, Bennett AK, Mastrodomenico V. 2018. Tools for Rapid Genetic Engineering of Vibrio fischeri. Appl Environ Microbiol. 84(14):e00850-18. doi:10.1128/AEM.00850-18.

Widney, 2024. Evolution of novel metabolic pathways. Department of Biochemistry. Graduate school of Arts and Sciences University of Colorado at Boulder.

Widney KA, Yang D-D, Rusch LM, Copley SD. 2024. CRISPR-Cas9-assisted genome editing in E. coli elevates the frequency of unintended mutations. :2024.03.19.584922. doi:10.1101/2024.03.19.584922.

Zhang W, Zhang M, Gao C, Zhang Yipeng, Ge Y, Guo S, Guo X, Zhou Z, Liu Q, Zhang Yingxin, et al. 2017. Coupling between d-3-phosphoglycerate dehydrogenase and d-2-hydroxyglutarate dehydrogenase drives bacterial l-serine synthesis. Proc Natl Acad Sci U S A. 114(36):E7574–E7582. doi:10.1073/pnas.1619034114.

Zhang Z, Peng H, Yang D, Zhang G, Zhang J, Ju F. 2022. Polyvinyl chloride degradation by a bacterium isolated from the gut of insect larvae. Nat Commun. 13(1):5360. doi:10.1038/s41467-022-32903-y.

Zhao G, Winkler ME. 1996. A novel alpha-ketoglutarate reductase activity of the serA-encoded 3-phosphoglycerate dehydrogenase of Escherichia coli K-12 and its possible implications for human 2-hydroxyglutaric aciduria. J Bacteriol. 178(1):232–239. doi:10.1128/jb.178.1.232-239.1996.

Zimmermann J, Werner E, Sodei S, Moran J. 2024. Pinpointing Conditions for a Metabolic Origin of Life: Underlying Mechanisms and the Role of Coenzymes. Acc Chem Res. 57(20):3032–3043. doi:10.1021/acs.accounts.4c00423.

Appendix

Table A-1. Strains used in this work.

Strain	Genotype	Notes
E. coli **DH5α lambda pir**		Obtained from Dr. Eric Stabb
E. coli **NiCO21**		Obtained from Dr. Karl Widney
E. coli **NiCO21** ***thrB::cmR***	NiCO21 with thrB replaced with cmR	Engineered by Cat Simmons
E. coli **BL21**		Engineered by Dr. Juhan Kim
E. coli **mu free donor lambda pir (MFD)**	MG1655 RP4-2-Tc::[ΔMu1::*aac(3)IV*-Δ*aphA*-Δ*nic35*-Δ*Mu2*::*zeo*] Δ*dapA*::(*erm-pir*) Δ*recA*	obtained from Dr. Aaron Whiteley; from (Ferrières et al., 2010)
JK1069	*E. coli* BL21 *pdxB*::*cmR serA*::*cmR*	Engineered by Dr. Juhan Kim. Used for SerA protein expression
Aliivibrio fischeri **ES114**		Obtained from Dr. Eric Stabb
KW087	*A. fischeri* ES114 *pdxB*::*kanR*	Engineered by Dr. Karl Widney, parental strain for TMM/glucose evolution
Af2	*A. fischeri* ES114 *pdxB*::*kanR serA** L19F	*serA* Mutant strain evolved in TMM/glucose. Engineered by Dr. Karl Widney
Af1	*A. fischeri* ES114 *pdxB*::*kanR yidA** E83*	*yidA* Mutant strain evolved in TMM/glucose. Engineered by Dr. Karl Widney
LP009	*A. fischeri thrB*::*cmR*	Used for growth assays
LP011	*Af2 thrB*::*cmR*	Used for growth assays
LP012	*Af1 thrB*::*cmR*	Used for growth assays
LP039	*A. fischeri serA*::*cmR*	Used for growth assays
LP043	*A. fischeri serC*::*cmR*	Used for growth assays
LP046	*Af1 serA*::*cmR*	Used for growth assays
LP051	*Af1 serC*::*cmR*	Used for growth assays
LP056	*Af2 serA*::*cmR*	Used for growth assays
LP057	*Af2 serC*::*cmR*	Used for growth assays
LP097	*A. fischeri aspC*::*emR*	Used for growth assays
LP101	*Af1 aspC*::*emR*	Used for growth assays
LP104	*Af2 aspC*::*emR*	Used for growth assays
LP108	*A. fischeri serC*::*cmR aspC*::*emR*	Used for growth assays
LP111	*Af2 serC*::*cmR aspC*::*emR*	Used for growth assays
LP122	*Af1 serC*::*cmR aspC*::*emR*	Used for growth assays

Table A-2. Plasmids used in this work.

Plasmid	Use/Description	Source/Reference
pHGDH	expression of D2HGDH with N-terminal 6xHis-tag under control of lac promoter; pET28 backbone, confers kanamycin resistance	(J. Kim et al., 2019)
pETFAB	expression of ETF A and ETF B with N-terminal 6xHis-tag under control of lac promoter; pET28 backbone, confers kanamycin resistance	(J. Kim et al., 2019)
pEVS94	suicide cloning vector; used as template to amplify erythromycin resistance	(Stabb & Ruby, 2002)
pKAW002	Cloning vector bb used for PCR amplification of genes, confers chloramphenicol resistance.	
pLostfoX-Kan	helper plasmid for performing linear deletion protocol in *A. fischeri*, confers kanamycin resistance	(Brooks et al., 2014)
pLostfoX-Gm	helper plasmid for performing linear deletion protocol in *A. fischeri*, confers gentamycin resistance	This work
pLCP005, pLCP006	pLCP005 was an intermediate plasmid in the production of pLCP006; pLCP006 harbours linear editing cassette for deletion of *serA* in *A. fischeri* containing chlor with 1.5 kbp homology arms flanking *A. fischeri serA*; pMB1 origin of replication; confers ampicillin and chloramphenicol resistance	This work
pLCP007, pLCP008	pLCP007 was an intermediate plasmid in the production of pLCP008; pLCP008 harbours linear editing cassette for deletion of *serC* in *A. fischeri* containing *cmR* with 1.5 kbp homology arms flanking *A. fischeri serC*; pMB1 origin of replication; confers ampicillin and chloramphenicol resistance	This work
pLCP015, pLCP016, pLCP01	pLCP015 and pLCP016 were intermediate plasmids in the production of pLCP017; pLCP017 harbours linear editing cassette for deletion of *aspC* in *A. fischeri* containing erm with 1.5 kbp homology arms flanking *A. fischeri aspC*; pMB1 origin of replication; confers ampicillin and erythromycin resistance	This work
pLCP013	expression of *A. fischeri* ThrB with N-terminal 6xHis-tag under control of lac promoter; pET28 backbone, kanamycin resistance	This work

pKAW050	expression of *A. fischeri* SerA with N-terminal 6xHis-tag under control of lac promoter; pET28 backbone, kanamycin resistance	Constructed by Dr. Karl Widney
pKAW051	expression of *A. fischeri* SerA* L19F with N-terminal 6xHis-tag under control of lac promoter; pET28 backbone, kanamycin resistance	Constructed by Dr. Karl Widney
pLCP022	expression of *A. fischeri* SerA* C23Y with N-terminal 6xHis-tag under control of lac promoter; pET28 backbone, kanamycin resistance	This work
pLCP023	expression of *A. fischeri* SerA* S296A with N-terminal 6xHis-tag under control of lac promoter; pET28 backbone, kanamycin resistance	This work
pLCP024	expression of *A. fischeri* SerA* V330Ewith N-terminal 6xHis-tag under control of lac promoter; pET28 backbone, kanamycin resistance	This work
pLCP019	expression of *P. putida* SerA with N-terminal 6xHis-tag under control of lac promoter; pET28 backbone, kanamycin resistance	This work
pLCP021	expression of *A. baylei* SerA with N-terminal 6xHis-tag under control of lac promoter; pET28 backbone, kanamycin resistance	This work
pLCP025	expression of *S. enterica* SerA with N-terminal 6xHis-tag under control of lac promoter; pET28 backbone, kanamycin resistance	Constructed by Dr. Dong-Dong Yang
pLCP027	expression of *E. coli* SerA* ΔL351with N-terminal 6xHis-tag under control of lac promoter; pET28 backbone, kanamycin resistance	This work
pLCP028	expression of *E. coli* SerA* ΔN355 with N-terminal 6xHis-tag under control of lac promoter; pET28 backbone, kanamycin resistance	This work
JK1081	expression of *E. coli* SerA with N-terminal 6xHis-tag under control of lac promoter; pET28 backbone, kanamycin resistance	(J. Kim et al., 2019)
JK1082	expression of *E. coli* SerA* V16G with N-terminal 6xHis-tag under control of lac promoter; pET28 backbone, kanamycin resistance	(J. Kim et al., 2019)
JK1083	expression of *E. coli* SerA* +403G with N-terminal 6xHis-tag under control of lac	(J. Kim et al., 2019)

	promoter; pET28 backbone, kanamycin resistance	
JK1084	expression of *E. coli* SerA* S296A with N-terminal 6xHis-tag under control of lac promoter; pET28 backbone, kanamycin resistance	(J. Kim et al., 2019)
JK1085	expression of *E. coli* SerA* +381MV with N-terminal 6xHis-tag under control of lac promoter; pET28 backbone, kanamycin resistance	(J. Kim et al., 2019)
JK1086	expression of *E. coli* SerA* I304L with N-terminal 6xHis-tag under control of lac promoter; pET28 backbone, kanamycin resistance	(J. Kim et al., 2019)
JK1087	expression of *E. coli* SerA* L47S with N-terminal 6xHis-tag under control of lac promoter; pET28 backbone, kanamycin resistance	(J. Kim et al., 2019)
JK1088	expression of *E. coli* SerA* VQ370P, ΔT371 with N-terminal 6xHis-tag under control of lac promoter; pET28 backbone, kanamycin resistance	(J. Kim et al., 2019)
JK1089	expression of *E. coli* SerA* T63N with N-terminal 6xHis-tag under control of lac promoter; pET28 backbone, kanamycin resistance	(J. Kim et al., 2019)
JK1090	expression of *E. coli* SerA* G377Cwith N-terminal 6xHis-tag under control of lac promoter; pET28 backbone, kanamycin resistance	(J. Kim et al., 2019)

Table A-3. Primers that were used in this work. Blue and red signify a 2 0nt overhang used for SOE PCR or Gibson Assembly.

Name	Sequence	Use
LP005	TTATGTTATACAGCTTCATATTACGCCCCGCCCTGCCACT	Amplification primers for the chloramphenicol resistance cassette to delete *thrB* in *A. fischeri*. Primers used in SOE PCR. Red 20nt overhang upstream homology arm; blue, 20nt overhang upstream homology arm
LP006	TTGGAAATTAGGAGTATAGACCTGGTGTCCCTGTTGATACCG	
LP007	CTGTGCGTTTTAACTCTCTAA	Amplification primers for the upstream homology arm to delete *thrB* in *A. fischeri* with *cmR*; LP007 and LP010 were used to amplify the editing cassette after the SOE PCR
LP008	AGTGGCAGGGCGGGGCGTAATATGAAGCTGTATAACATAAAAGAAAATG	
LP009	GTATCAACAGGGACACCAGGTCTATACTCCTAATTTCCAACCAAGC	Amplification primers for the downstream homology arm to delete *thrB* in *A. fischeri* with *cmR*; LP007 and LP010 were used to amplify the editing cassette after the SOE PCR
LP010	CCGGTGAAGATAATCTGGCTATTAA	
KW434	CCGCTACATCTTTATCTTTGCATATAC	internal primers used in Colony PCR to screen for the deletion of *thrB* in *A. fischeri*
KW435	TTATGCTCCTGCATCAATAGGAAAT	
LP011	GGTGAACGCATTTCTATTGTCATG	External primers used in Colony PCR to screen for the deletion of *thrB* in *A. fischeri*
LP012	CCGTGATGTTGCTATCGAAAAAG	
LP027	ATTAAAGATGGCGAGAACGC	Primers used for Sanger sequencing to verify the deletion of *thrB* in *A. fischeri*
LP028	TAAAATCCTCAGCAAGAAGTGC	
LP061	AGGCGTATCACGAGGCCCTTGTCGTAACGCTTTATCTCCTATTG	Amplification primers for the upstream homology arm to delete *serA* in *A. fischeri* with *cmR*; Primers used in Gibson Assembly. Blue, 20 nt overhang with backbone; red, 20 nt overhang for with chloramphenicol resistance casette
LP062	GTATCAACAGGGACACCAGGGGTCGTTCTTATCCTTAAAAACAAAATTATG	
LP063	TTTTAAGGATAAGAACGACCCCTGGTGTCCCTGTTGATACCG	Amplification for the chloramphenicol resistance cassette to delete *serA* in *A. fischeri* with *cmR*; Primers used in Gibson Assembly. Blue, 20 nt overhang with upstream homology
LP064	CTCACATGTTCTTTCCTGCGTTACGCCCCGCCCTGCCACT	

		arm; red, 20 nt overhang with backbone
LP065	AGTGGCAGGGCGGGGCGTAAGATAAATAAAAAATGGGCAGCTTAATTAGCTG	Amplification primers for the downstream homology arm to delete *serA* in *A. fischeri* with *cmR*; Primers used in Gibson Assembly. Blue, 20 nt overhang with chloramphenicol resistance gene; red, 20 nt overhang with backbone
LP066	CTCACATGTTCTTTCCTGCGTCACACTCTTGTTCGTTACCTTTTATTC	
LP067	GGTAACGAACAAGAGTGTGACGCAGGAAAGAACATGTGAGCAAAAGG	amplification primers of the backbone from pLCP005
LP068	CTGCCCATTTTTTATTTATCTTACGCCCCGCCCTGCCACT	
LP029	TCACACTCTTGTTCGTTACC	Reamplification of the *A. fischeri serC* linear DNA fragment deletion cassette from pLCP006
LP030	GTCGTAACGCTTTATCTCCT	
KW444	TTGTGTTGAAGTTTTCCAAGCAGA	internal primers used in Colony PCR to screen for the deletion of *serA* in *A. fischeri*
KW465	TCAACATCAATAACAACATAGCCCAT	
LP035	GGGGTATTCCATGACATCTC	External primers used in Colony PCR to screen for the deletion of *serA* in *A. fischeri*
LP036	GTAGCGAACAGTGTAAGTAAC	
LP037	ATTCCGTAATTTTCTTACCC	Primers used for Sanger sequencing to verify the deletion of *serA* in *A. fischeri*
LP038	GATTTCTGACTCTGTATCTG	
LP069	GTATCAACAGGGACACCAGGGTTTCTTAAAACTCCTGTTGATGTTTACA	Amplification primers for the upstream homology arm to delete *serC* in *A. fischeri* with *cmR*; Primers used in Gibson Assembly. Blue, 20 nt overhang with backbone; red, 20 nt overhang with chloramphenicol resistance cassette
LP070	AGGCGTATCACGAGGCCCTTGATAACGTTGGATAACAATATGAACGAG	
LP071	CAACAGGAGTTTTAAGAAACCCTGGTGTCCCTGTTGATACCG	Amplification primers for chloramphenicol resistance cassette to delete *serC* in *A. fischeri*; Primers used in Gibson Assembly. Blue, 20 nt overhang with upstream homology arm; red, 20 nt overhang with backbone
LP072	CTCACATGTTCTTTCCTGCGTTACGCCCCGCCCTGCCACT	
LP073	CTCACATGTTCTTTCCTGCGCTTCTTTAAGAAACTAATACCGCTTATCC	Amplification primers for the downstream homology arm to delete *serC* in *A. fischeri* with *cmR*; Primers used in Gibson Assembly. Blue, 20 nt overhang
LP074	AGTGGCAGGGCGGGGCGTAAGTATTGCTCTTATTAACTGATACGAAAAAGC	

		with chloramphenicol resistance casette; red, 20 nt overhang for with backbone
LP075	TCAGTTAATAAGAGCAATACTTACG CCCCGCCCTGCCACT	Amplification of the backbone from the intermediate plasmid pLCP007
LP076	GTATTAGTTTCTTAAAGAAGCGCAG GAAAGAACATGTGAGCAAAAGG	
LP039	GATAACGTTGGATAACAATATG	Amplification of the *A. fischeri serC* linear deletion cassette from pLCP008
LP040	CTTCTTTAAGAAACTAATACCG	
LP045	GTTACCAGTAGACGTTCTCG	Internal primers used in Colony PCR to screen for the deletion of *serC* in *A. fischeri*
LP046	CATAAATTGCACAAGCGCTTC	
LP047	AGAGTTGTGTTGGGCTTATTGTG	External primers used in Colony PCR to screen for the deletion of *serC* in *A. fischeri*
LP048	TGGGGCGAACGTGTTGTTAG	
LP049	GTGAAATAGATCACTTTCTG	Primers used for Sanger sequencing to verify the deletion of *serC* in *A. fischeri*
LP050	CAACGCTTTTAATTACCTTAG	
LP111	GTATCAACAGGGACACCAGGCCAT GGTGTAAGTAAAATAAAAGAGTTA G	Amplification primers of the upstream homology arm to delete aspC in *A. fischeri* with *emR*; Primers used in Gibson Assembly. Blue, 20 nt overhang for Gibson Assembly with backbone; red, 20 nt overhang for Gibson Assembly with chloramphenicol resistance casette
LP112	AGGCGTATCACGAGGCCCTTACATA AATGAATACAATTTCACTCATTCTC	
LP113	TTATTTTACTTACACCATGGCCTGGT GTCCCTGTTGATACCG	Amplification primers for the chloramphenicol resistance cassette to delete *aspC* in *A. fischeri* with *cmR*. Primers used in Gibson Assembly. Blue, 20 nt overhang with upstream homology arm; red, 20 nt overhang with backbone
LP114	CTCACATGTTCTTTCCTGCGTTACGC CCCGCCCTGCCACT	
LP115	AGTGGCAGGGCGGGGCGTAACGCA GGAAAGAACATGTGAGCAAAAGG	Amplification of the backbone from pT2SCb to create pLCP015; Primers used in Gibson assembly. Blue, 20 nt overhang with chloramphenicol resistance cassette; red, 20 nt overhang with the upstream homology arm
LP116	GAAATTGTATTCATTTATGTAAGGG CCTCGTGATACGCCT	
LP117	CTTACAATTACTTCTGATTCTTACGC CCCGCCCTGCCACT	

LP118	TCAATGGCTACAAGATCAGACGCA GGAAAGAACATGTGAGCAAAAGG	Amplification primers for the backbone of the intermediate plasmid pLCP015
LP119	CTCACATGTTCTTTCCTGCGTCTGAT CTTGTAGCCATTGATG	Amplification primers for the downstream homology arm to create the linear DNA fragment to delete aspC in *A.fischeri* serC. Primers used in Gibson assembly. Blue, 20 nt overhang with chloramphenicol resistance gene; red, 20 nt overhang with backbone
LP120	AGTGGCAGGGCGGGGCGTAAGAAT CAGAAGTAATTGTAAGACATAGAA AAG	
LP145	TTATTTTACTTACACCATGGAACTT AAGAGTGTGTTGATAGTGCAGTATC T	Amplification primers of an erythromycin resistance cassette to replace the *cmR* in pLCP016 and create pLCP017 with *emR*. Primers used in Gibson assembly. blue, 20 nt overhang with downstream homology arm; red, 20 nt overhang with downstream homology arm
LP146	CTTACAATTACTTCTGATTCTTTAGC TCCTTGGAAGCTGTCAG	
LP147	TATCAACACACTCTTAAGTTCCATG GTGTAAGTAAAATAAAAGAGTTAG	Amplification primers for the backbone pLCP016 used to create pLCP017. Primers used in Gibson assembly. blue, 20 nt overhang with beginning of erythromycin resistance gene; red, 20 nt overhang with end of erythromycin resistance gene
LP148	ACAGCTTCCAAGGAGCTAAAGAAT CAGAAGTAATTGTAAGACATAGAA AAG	
LP125	ACATAAATGAATACAATTTCACTCA TTCTCATT	Amplification primers to create the *A. fischeri aspC* linear deletion fragment from pLCP017
LP126	TCTGATCTTGTAGCCATTGATGC	
LP123	TACCAGCAACACTGATACGG	Internal primers used for Colony PCR to screen for deletion of *aspC* in *A. fischeri*
LP124	GACCCTCGTGCTGAAAAAAT	
LP121	AGACATACATGGTTTGCTCATCC	External primers used in Colony PCR to screen for the deletion of *aspC* in *A. fischeri*
LP122	GCAACCGATGCAGATGTCAT	
LP149	CGTTACCTAACCGTTGCAAAC	Primers used in sanger sequencing to confirm the deletion of *aspC* in *A. fischeri strains*
LP150	GCTAAGAAAGTGTGAAACTGGC	
LP155	ACCTGTACTTCCAGGGATCCATGAG CAAGACTTCTCTCGACAAGAG	Amplification primers of the serA gene in *P. putida* to construct the pLCP019 SerA protein expression plasmid
LP156	CCGCAAGCTTGGCTGCAGGTTTAGA ACAGGACGCGCGAAC	
LP159	ACCTGTACTTCCAGGGATCCATGAG CCAACATCTATCACTACCT	Amplification primers of the serA gene in *A. fischeri* to construct the

LP160	CCGCAAGCTTGGCTGCAGGTTTAGAACAGAACGCGAACGC	pLCP022, pLCP023, and pLCP024 SerA protein expression plasmids
LP161	ACCTGTACTTCCAGGGATCCATGGCAAAGGTATCGCTGGAGAAAGAC	Amplification primers of the serA gene in *A. baylyi* to construct the pLCP021 SerA protein expression plasmid
LP162	CCGCAAGCTTGGCTGCAGGTTTAGTACAGCAGACGGGCGCG	
KW232	ACCTGTACTTCCAGGGATCCGCAAAAGTATCTCTGGAAAAG	Amplification primers of the serA gene in *E. coli* to construct the pLCP027 and pLCP028 SerA protein expression plasmids
KW233	CCGCAAGCTTGGCTGCAGGTTTAATGAAGAATTCGAGCGC	

Figures

SerA enzymes used in the assays listed in Chapter II and Chapter IV are displayed below.

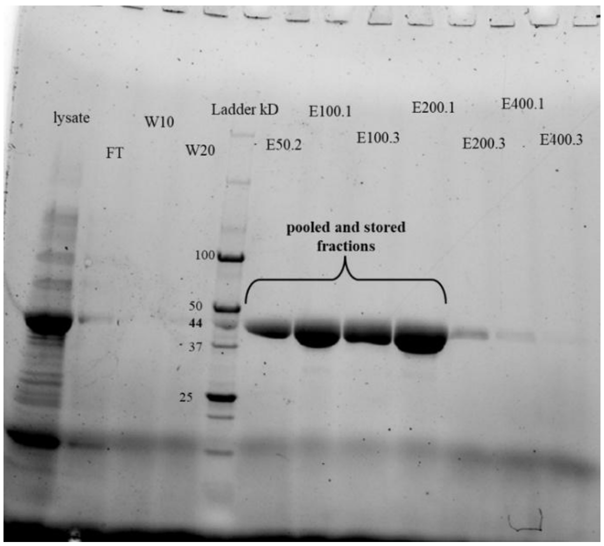

Figure A-1. SDS-page gel of fractions collected during purification of his-tagged wild-type *A. fischeri* SerA following IMAC. SerA protein is about 44 kD.

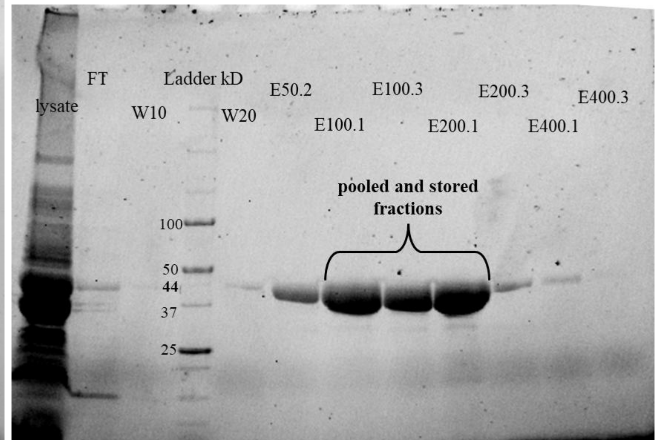

Figure A-2. SDS-page gel of fractions collected during purification of his-tagged mutated *A. fischeri* SerA L19F following IMAC. SerA protein is about 44 kD.

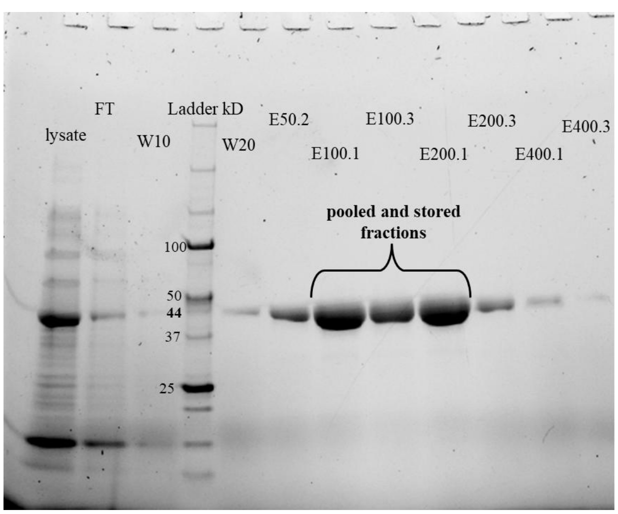

Figure A-3. SDS-page gel of fractions collected during purification of his-tagged mutated *A. fischeri* SerA C23Y following IMAC. SerA protein is about 44 kD.

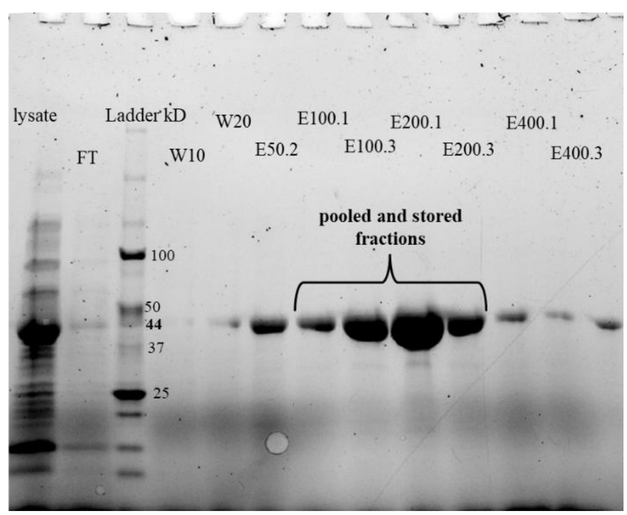

Figure A-4. SDS-page gel of fractions collected during purification of his-tagged mutated *A. fischeri* SerA S296A following IMAC. SerA protein is about 44 kD.

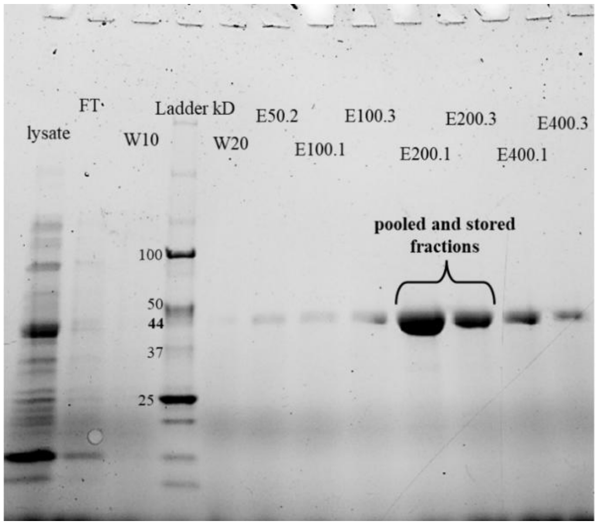

Figure A-5. SDS-page gel of fractions collected during purification of his-tagged mutated *A. fischeri* SerA V330E following IMAC. SerA protein is about 44 kD.

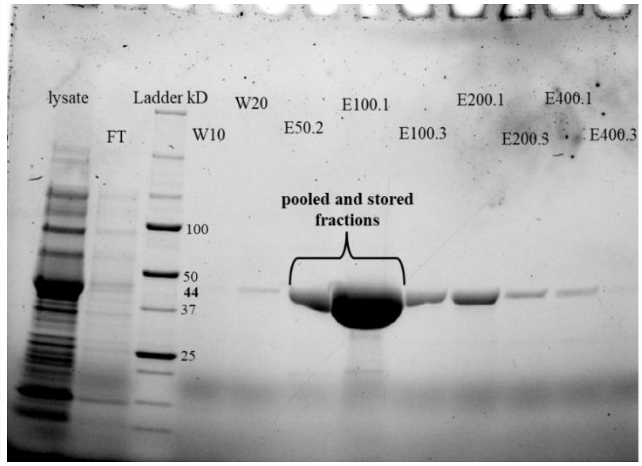

Figure A-6. SDS-page gel of fractions collected during purification of his-tagged wild-type *E. coli* SerA following IMAC. SerA protein is about 44 kD.

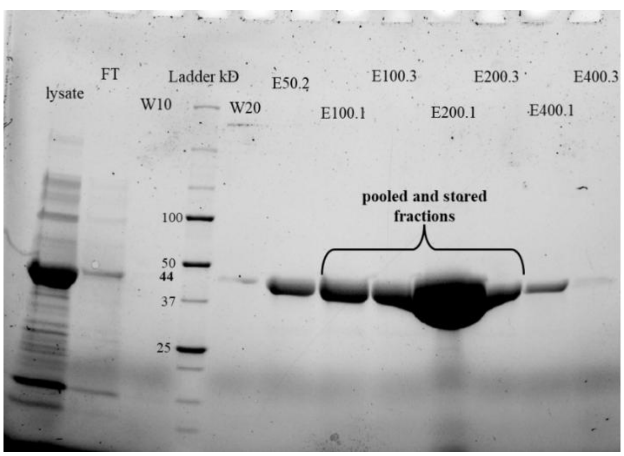

Figure A-7. SDS-page gel of fractions collected during purification of his-tagged mutated *E. coli* SerA V16G following IMAC. SerA protein is about 44 kD.

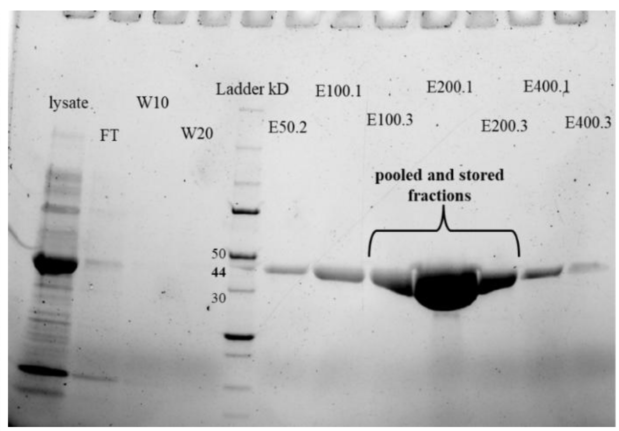

Figure A-8. SDS-page gel of fractions collected during purification of his-tagged mutated *E. coli* SerA +403G following IMAC. SerA protein is about 44 kD.

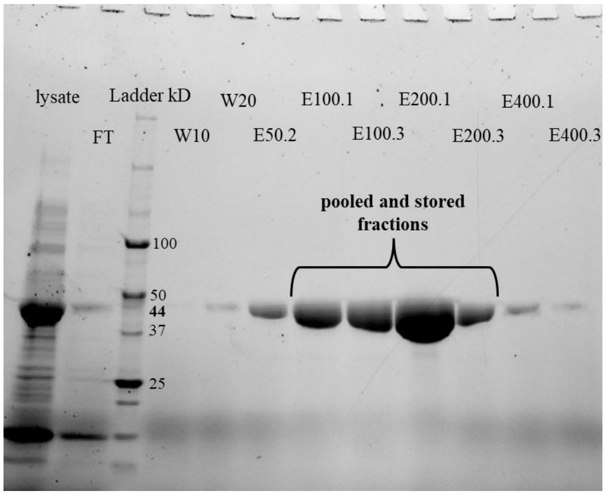

Figure A-9. SDS-page gel of fractions collected during purification of his-tagged mutated *E. coli* SerA S296A following IMAC. SerA protein is about 44 kD.

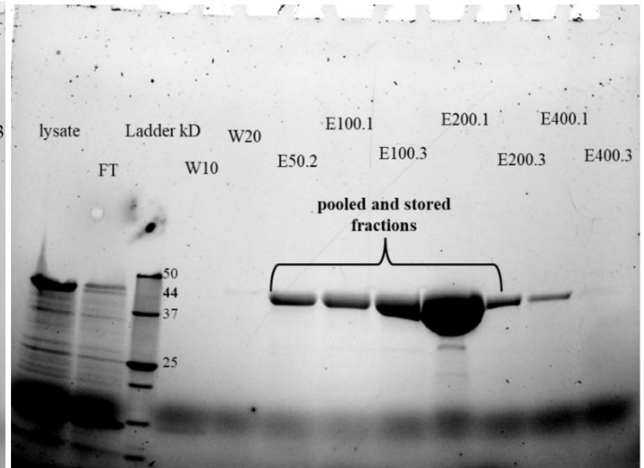

Figure A-10. SDS-page gel of fractions collected during purification of his-tagged mutated *E. coli* SerA +381MV following IMAC. SerA protein is about 44 kD.

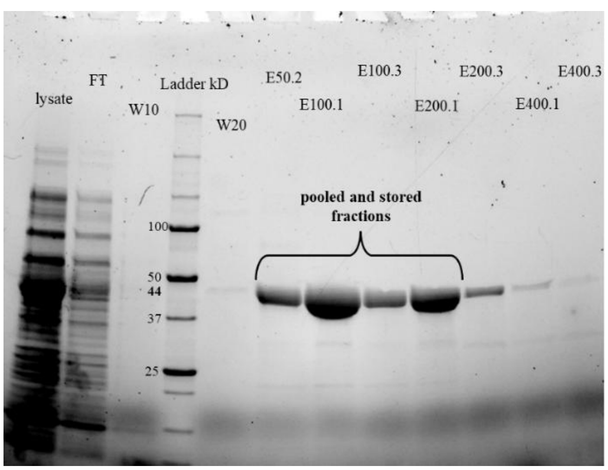

Figure A-11. SDS-page gel of fractions collected during purification of his-tagged mutated *E. coli* SerA I304L following IMAC. SerA protein is about 44 kD.

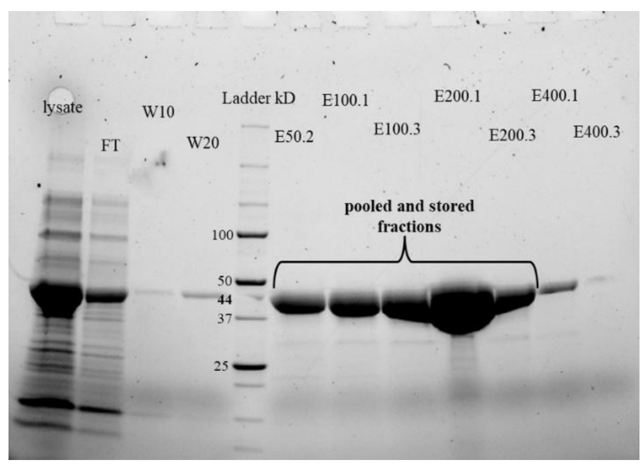

Figure A-12. SDS-page gel of fractions collected during purification of his-tagged mutated *E. coli* SerA L47S following IMAC. SerA protein is about 44 kD.

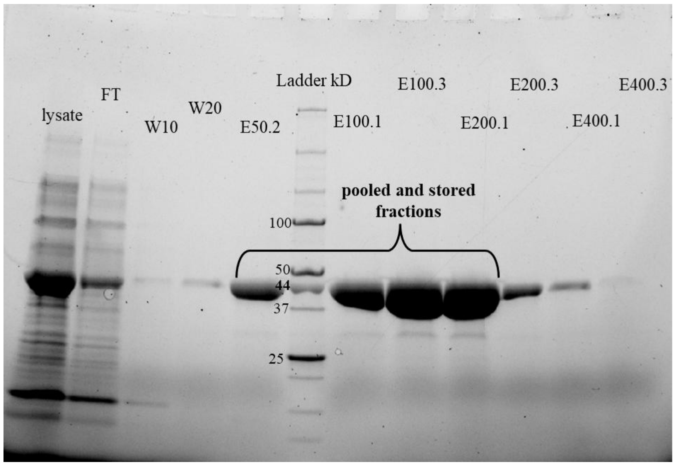

Figure A-13. SDS-page gel of fractions collected during purification of his-tagged mutated *E. coli* SerA Q370P ΔT371 following IMAC. SerA protein is about 44 kD.

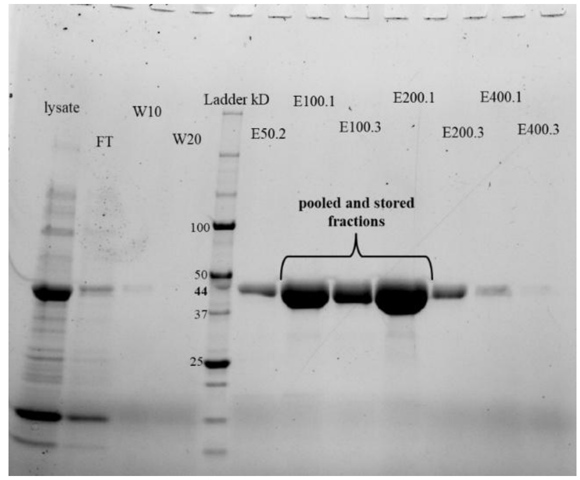

Figure A-14. SDS-page gel of fractions collected during purification of his-tagged mutated *E. coli* SerA T63N following IMAC. SerA protein is about 44 kD.

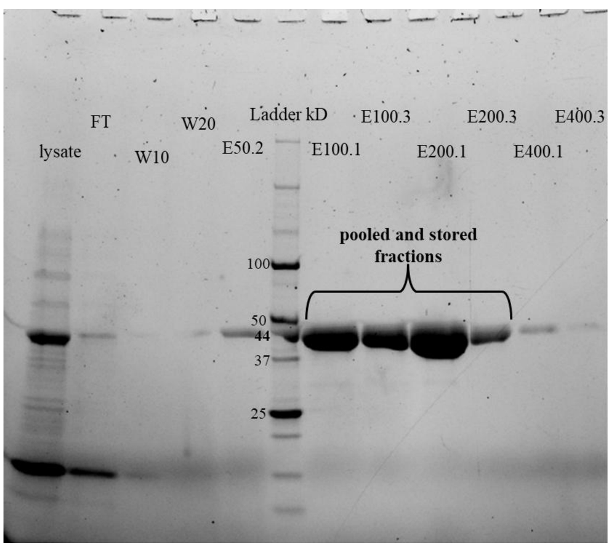

Figure A-15. SDS-page gel of fractions collected during purification of his-tagged mutated *E. coli* SerA G377C following IMAC. SerA protein is about 44 kD.

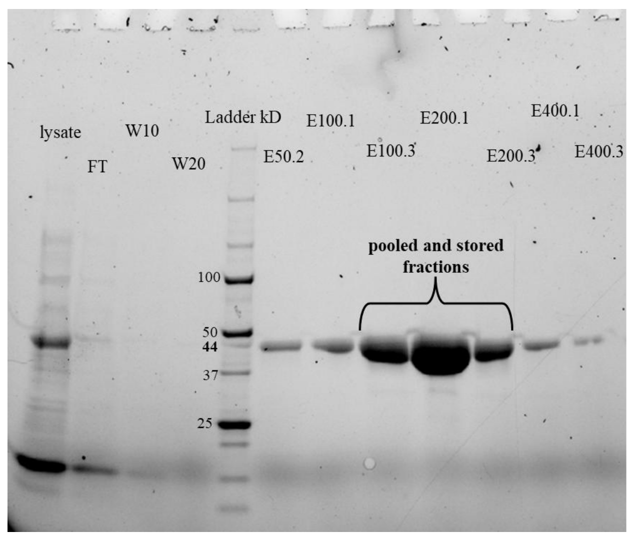

Figure A-16. SDS-page gel of fractions collected during purification of his-tagged mutated *E. coli* SerA ΔL351following IMAC. SerA protein is about 44 kD.

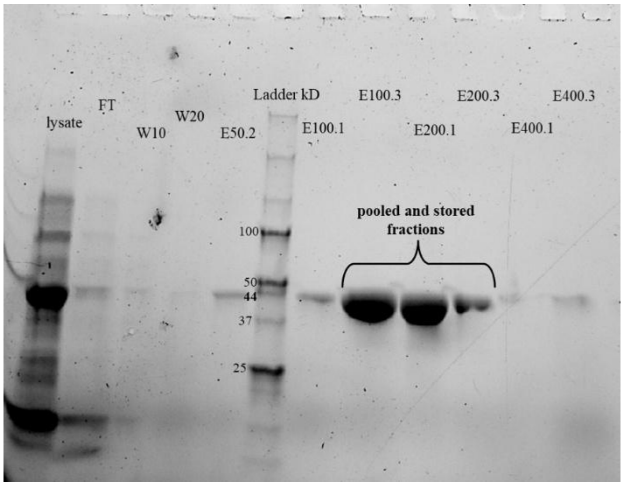

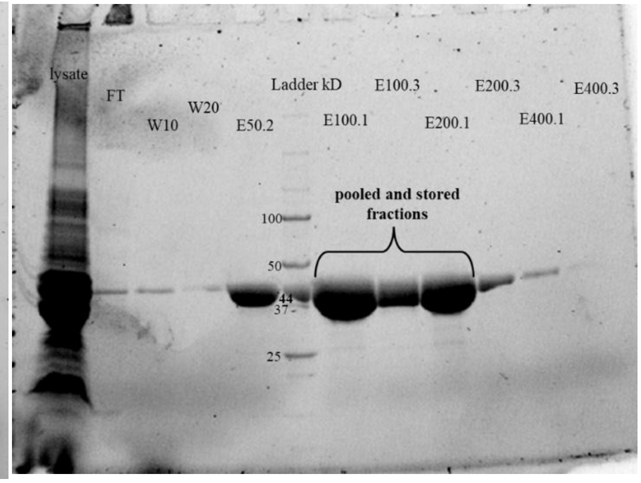

Figure A-14. SDS-page gel of fractions collected during purification of his-tagged mutated *E. coli* SerA ΔL355 following IMAC. SerA protein is about 44 kD.

Figure A-6. SDS-page gel of fractions collected during purification of his-tagged wild-type *P. putida* SerA following IMAC. SerA protein is about 44 kD.

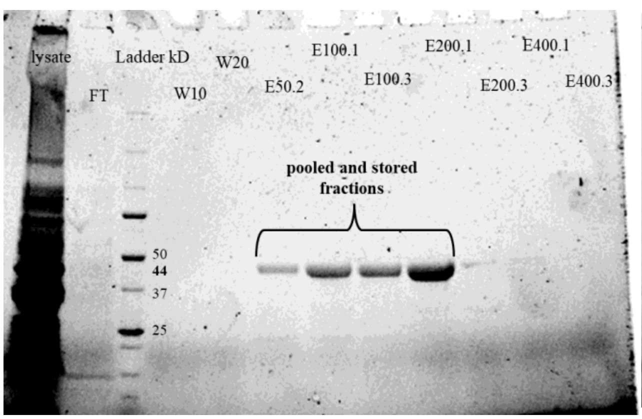

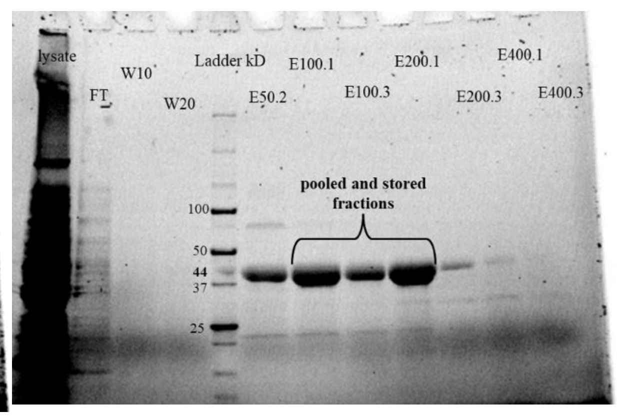

Figure A-19. SDS-page gel of fractions collected during purification of his-tagged wild-type *S. enterica* SerA following IMAC. SerA protein is about 44 kD.

Figure A-20. SDS-page gel of fractions collected during purification of his-tagged wild-type *A. baylyi* SerA following IMAC. SerA protein is about 44 kD.